

Accepted Manuscript

Design, synthesis and apoptosis inducing effect of novel (Z)-3-(3'-methoxy-4'-(2-amino-2-oxoethoxy)-benzylidene)indolin-2-ones as potential antitumor agents

Kishna Ram Senwar, T. Srinivasa Reddy, Dinesh Thummuri, Pankaj Sharma, V.G.M. Naidu, Gannaju Srinivasulu, Nagula Shankaraiah



PII: S0223-5234(16)30310-5

DOI: [10.1016/j.ejmech.2016.04.025](https://doi.org/10.1016/j.ejmech.2016.04.025)

Reference: EJMECH 8540

To appear in: *European Journal of Medicinal Chemistry*

Received Date: 10 December 2015

Revised Date: 3 March 2016

Accepted Date: 8 April 2016

Please cite this article as: K.R. Senwar, T.S. Reddy, D. Thummuri, P. Sharma, V.G.M. Naidu, G. Srinivasulu, N. Shankaraiah, Design, synthesis and apoptosis inducing effect of novel (Z)-3-(3'-methoxy-4'-(2-amino-2-oxoethoxy)-benzylidene)indolin-2-ones as potential antitumor agents, *European Journal of Medicinal Chemistry* (2016), doi: 10.1016/j.ejmech.2016.04.025.

This is a PDF file of an unedited manuscript that has been accepted for publication. As a service to our customers we are providing this early version of the manuscript. The manuscript will undergo copyediting, typesetting, and review of the resulting proof before it is published in its final form. Please note that during the production process errors may be discovered which could affect the content, and all legal disclaimers that apply to the journal pertain.

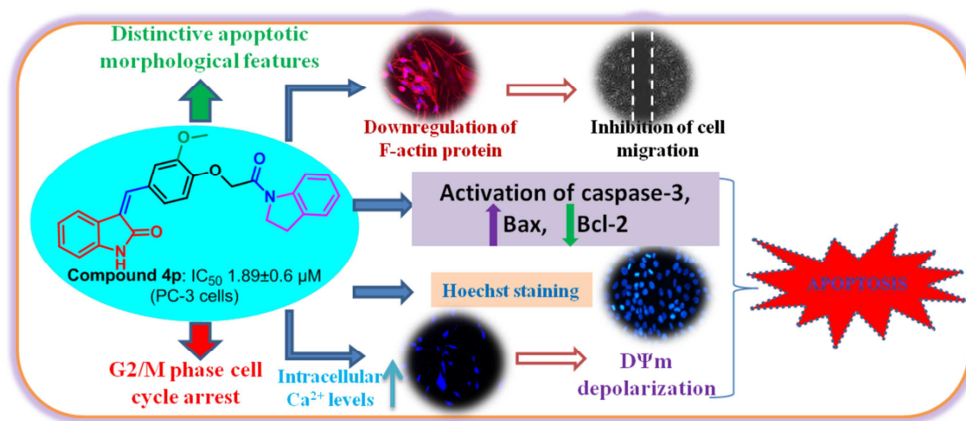
Graphical Abstract

Design, synthesis and apoptosis inducing effect of novel (Z)-3-(3'-methoxy-4'-(2-amino-2-oxoethoxy)-benzylidene)indolin-2-ones as potential antitumor agents

Kishna Ram Senwar,^a T. Srinivasa Reddy,^a Dinesh Thummuri,^b Pankaj Sharma,^a V. G. M. Naidu,^b Gannaju Srinivasulu,^a Nagula Shankaraiah^{a*}

^aDepartment of Medicinal Chemistry, National Institute of Pharmaceutical Education and Research (NIPER) Hyderabad 500 037, India

^bDepartment of Pharmacology and Toxicology, National Institute of Pharmaceutical Education and Research (NIPER) Hyderabad 500 037, India



Design, synthesis and apoptosis inducing effect of novel (Z)-3-(3'-methoxy-4'-(2-amino-2-oxoethoxy)-benzylidene)indolin-2-ones as potential antitumor agents

Kishna Ram Senwar,^a T. Srinivasa Reddy,^a Dinesh Thummuri,^b Pankaj Sharma,^a V. G. M. Naidu,^b Gannoju Srinivasulu,^a Nagula Shankaraiah^{a*}

^a*Department of Medicinal Chemistry, National Institute of Pharmaceutical Education and Research (NIPER) Hyderabad 500 037, India*

^b*Department of Pharmacology and Toxicology, National Institute of Pharmaceutical Education and Research (NIPER) Hyderabad 500 037, India*

*Corresponding author

Dr. Nagula Shankaraiah

Department of Medicinal Chemistry

National Institute of Pharmaceutical Education and Research

Hyderabad, 500037, India

Fax: (+91) 040 23073751

E-mail: shankar.niperhyd@gov.in; shankarnbs@gmail.com

Abstract

A series of new (Z)-3-(3'-methoxy-4'-(2-amino-2-oxoethoxy)benzylidene)indolin-2-one derivatives has been synthesized and evaluated for their cytotoxic activity against selected human cancer cell lines of prostate (PC-3 and DU-145), breast (BT-549 and MDA-MB-231) and non-tumorigenic prostate epithelial cells (RWPE-1). Among the tested, one of the compounds **4p** exhibited potent cytotoxicity selectively on prostate cancer cell lines (PC-3 and DU-145; IC₅₀: 1.89±0.6 and 1.94±0.2 μM, respectively). Further experiments were conducted with **4p** on PC-3 cancer cells to study the mechanisms of growth inhibition and apoptosis inducing effect. Treatment of PC-3 cells with test compound **4p** resulted in inhibition of cell migration through disorganization of F-actin protein. The flow-cytometry analysis results showed that the compound arrested PC-3 cancer cells in the G2/M phase of cell cycle in a dose dependent manner. Hoechst staining and annexin-V binding assay revealed that the compound **4p** inhibited tumor cell proliferation through induction of apoptosis. Western blot studies demonstrated that the compound **4p** treatment led to activation of caspase-3, increased expression of pro-apoptotic Bax and significantly decreased expression of anti-apoptotic Bcl-2 in human prostate cancer PC-3 cells. In addition, the mitochondrial membrane potential ($\Delta\Psi_m$) was also affected and the levels of intracellular Ca²⁺ were raised.

Key words:

Oxindole, Knoevenagel condensation, Benzylideneindolin-2-one, Heterocycles, Anticancer, Apoptosis

1.0. Introduction:

Cancer is one of the leading global health burden and most serious clinical problems in the world with increasing incidences every year. Despite avoiding behavioural risk factors such as tobacco, overweight and obesity, and preventive managements like dietary, medication and vaccination, the disease still affects millions of patients worldwide [1]. Most of the current anticancer drugs generally act on metabolically active or rapidly proliferating cells, and suffer from poor selectivity between normal and cancerous cells. The high toxicity and poor tolerance of the current anticancer drugs, highlighting the need to identify new molecules with potent antitumor activity, low toxicity and minimum side effects. Therefore, the design and synthesis of new chemical entities for the effective and safe cure of cancer are an active area of research in medicinal chemistry.

The indolin-2-one (oxindole) is a privileged scaffold, which represents an important class of heterocyclic compounds endowed of interesting pharmacological [2–5] and biological activities such as inhibitors of the MDM2-p53 interaction [6], antimicrobial [7], cholinesterases [8], histone deacetylases [9], and anticancer properties [10, 11]. Besides, sunitinib and nintedanib [Fig. 1] are the representative drugs emerged from this class and are in clinical use for targeted anticancer therapies [12]. The FDA approval of sunitinib and nintedanib paved the way to design and synthesis of various indolin-2-one based molecules with diverse activities against cancer [13, 14]. Particularly, the structural modifications at the C3- and C5-positions of the indolin-2-one ring have led many derivatives possessing increased antitumor activity. In this context, many synthetic indolin-2-one derivatives with anticancer activity were developed which inhibit diverse tyrosine and serine/threonine kinases, for instance, c-Met kinase [15], Pim kinase [16], RET kinase [17], FLT3 kinase [18], Aurora B kinase [19], glycogen synthase kinase-3 [20], cyclin-dependent kinases (CDKs) [21], and Polo-like kinase 4 (PLK4) [22]. Hence, we have previously reported the synthesis,

structure-activity relationship (SAR), and importance of 3-substituted-indolin-2-ones as well as spiro-fused-indolin-2-one based hybrids as potent cytotoxic agents [23–27].

On the other hand, incorporation of medicinally active moieties into a core bioactive natural product provides the means for accessing wider range of pharmacological profiles, especially in the area of anticancer therapeutics. For instance, various heterocyclic ring systems such as morpholine, pyrrolidine, piperidine, dimethylmorpholine, indoline *etc.* have been found as the fundamental scaffold components of several drugs in the market today [28, 29]. The significance of these moieties are well understood by medicinal chemists, since they play an important role in molecular properties or whole molecule properties such as three dimensionality, scaffold rigidity, lipophilicity or polarity, and can determine molecular reactivity, metabolic stability, cellular activity, and toxicity.

<insert Figure 1 here>

In our quest to develop more potent anticancer molecules, we integrated the structural features of representative examples of 3-alkenyl-indolin-2-ones by aiming at the identification of novel small molecules with potent antiproliferative effects on tumor cells. We hypothesized that the newly designed molecules comprising of 3-(3'-methoxybenzylidene)indolin-2-ones and saturated heterocyclic secondary amines connected through oxoethoxy-linker within a single molecule could enhance the cytotoxic activity that might work through induction of tumor cell apoptosis and cell cycle arrest. In this context, we herein reported the synthesis and *in vitro* anticancer evaluation of novel (Z)-3-(3'-methoxy-4'-(2-amino-2-oxoethoxy)-benzylidene)indolin-2-one derivatives with a view to produce the promising anticancer agents. Besides, we also explored the effects toward the cell cycle and possible mechanism of inducing apoptosis on human PC-3 cancer cells.

2.0. Results and Discussion

2.1. Chemistry

The (*Z*)-3-(3'-methoxy-4'-(2-amino-2-oxoethoxy)-benzylidene)indolin-2-one derivatives **4a–v** were synthesized by employing the Knoevenagel condensation between indolin-2-ones **7a–e** and the corresponding 3-methoxy-4-(2-amino-2-oxoethoxy)-benzaldehydes **11a–e** as shown in **Scheme 1**. Oxindoles **7a–e** were synthesized from the corresponding isatins through Wolff-Kishner reduction reaction with hydrazine-hydrate in the presence of potassium hydroxide. According to Sandmeyer's method, isatins **6a–e** were synthesized by converting the appropriate anilines **5a–e** into isonitrosoacetanilides *via* reaction with chloral hydrate and hydroxylamine hydrochloride followed by step-wise cyclization in acidic media. The respective key intermediates **11a–e** were synthesized from chloro-acetyl precursors **9a–e** by reacting with vanillin using potassium carbonate as a base. Alkylation of the vanillin with a variety of heterocyclic amines bearing oxoethoxy-linker introduced the basic functionalities and scope of diversity. Intermediates **9a–e** were synthesized from saturated heterocyclic secondary amines **8a–e**. Further, the (*Z*)-3-(3'-methoxy-4'-(2-amino-2-oxoethoxy)-benzylidene)indolin-2-ones bearing different heterocyclic secondary amines *viz.* morpholino, piperidin-1-yl, pyrrolidin-1-yl, indolin-1-yl, and 2,6-dimethylmorpholino were synthesized as title compounds **4a–v**. Finally, the compounds **4a–v** were unambiguously characterized by HRMS (ESI), ¹H and ¹³C NMR spectroscopy.

<insert Scheme 1 here>

2.1.1. Stereo-chemical characterization

The 3-alkenyl-indolin-2-ones were reported to exist as either *Z* or *E* isomer depending on the characteristics of the substituents at C3-position of indolin-2-one. Therefore, to establish the *E/Z* stereochemistry of the compounds **4a–v**, we considered the fact that *E* and *Z* isomers of

benzylidene-indolin-2-ones might have time dependent isomerization lability in polar solvent (*i.e.*, DMSO- d_6). The previous literature reports [30, 31] suggest that the *ortho* protons (C2'- or C6'-protons) of the benzylidene ring in *Z* isomer are deshielded relative to those in *E* isomer. The deshielding of C2'- or C6'-protons could be due to the presence of nearby C2-position carbonyl of indolin-2-one ring in the *Z* isomer form. As a result, the two isomer forms could be easily distinguished by ^1H and ^{13}C NMR analysis.

The stereochemistry was assigned for one of the representative compounds **4v** by detailed NOE studies. The ^1H and ^{13}C NMR assignments for compounds **4v** were carried out using gDQFCOSY, ROESY, HSQC and HMBC experiments in DMSO- d_6 at 25 °C on Bruker 500 MHz (for ^1H NMR) and 125 MHz (for ^{13}C NMR), respectively [see ESI[†]]. The presence of NOE between H4-H10, H10-H12 and H10-H16 in ROESY experiment conforms the geometry at double bond was characterized as *Z*-isomer as depicted in **Figure 2**.

<insert Figure 2 here>

2.2. Biological Evaluation

2.2.1. *In vitro* cytotoxic activity

All the synthesized compounds **4a–v** were evaluated for their *in vitro* antiproliferative activity against selected human cancer cell lines of prostate (PC-3 and DU-145), breast (BT-549 and MDA-MB-231) and normal human prostate epithelial cells (RWPE-1) by using 3-(4,5-dimethylthiazol-2-yl)-2,5-diphenyltetrazolium bromide (MTT) assay. Sunitinib was used as reference standard [32–35] and the *in vitro* screening results are summarized in **Table 1**. The results indicated that the compounds **4a**, **4f**, **4h**, **4i**, **4p**, **4q**, and **4t** exhibited significant cytotoxicity on both prostate cancer cells (PC-3 and DU-145) with IC_{50} values in the range of 1.89 ± 0.6 – 6.97 ± 0.6 μM . Gratifyingly, the compound **4p** was the most active compound in this series which exhibited potent cytotoxicity on PC-3 cancer cell line with IC_{50} of 1.89 ± 0.6 μM ,

whereas the reference standard sunitinib displayed IC_{50} of $19.6 \pm 3.0 \mu M$. The compounds showing significant cytotoxicity on prostate cancer cell lines (PC-3 and DU-145) were further tested for their *in vitro* cytotoxicity on non-tumorigenic prostate epithelial cells (RWPE-1), to determine the safety of these compounds against non cancer cells. It was interesting to observe that the tested compounds **4a**, **4f**, **4h**, **4i**, **4p**, **4q**, and **4t** were moderately selective toward cancer cells when compared to non cancer RWPE-1 cells.

From the analysis of IC_{50} values of these compounds, it is observed that most of the compounds were less potent against breast cancer cells, BT-549 and MDA-MB-231, respectively, except compound **4h** which is fairly selective towards BT-549 cells. In general, the cytotoxic activity decreases with heterocyclic ring substituents in the order of indolin-1-yl > piperidine-1-yl > 2,6-dimethylmorpholino > morpholino > pyrrolidin-1-yl. Indeed, the presence of indoline ring makes more contribution to the antitumor activity characterized with most active compounds **4p** and **4q**; while the derivatives with piperidine group (**4f-j**) show a reduced antiproliferative activity. Changing the piperidine ring with other heterocyclic ring substituents (*i.e.*, 2,6-dimethylmorpholine, morpholine and pyrrolidine) further reduces the *in vitro* cytotoxic activity. In addition, the introduction of electron-donating 3'-methoxy group on to benzylidene ring resulted in modest improvement in the potency and might be a potential location for further chemical modification. On the other hand, the activity profile of **4a**, **4f** and **4p** corroborates toward the preference of H-substituent on C5-position of indolin-2-one in comparison to C5-methyl as well as C5-halogen counterparts. Among halogenated analogues, the compounds with 5-chloro substitution (**4h** and **4t**) at C5-position of indolin-2-one are generally more active than the corresponding 5-fluoro (**4b**, **4g**, **4l** and **4s**) and 5-bromo analogs (**4d**, **4n** and **4u** except **4i**, which is equipotent to **4t**). Overall, the applicability of active compounds could not be questioned due to the

known toxicity of halogens, since the most promising compound **4p** bearing no halogen substituent.

From the structure activity relationships (SARs), it could be inferred in general that the modifications on the benzylidene ring as well as C5-position of indolin-2-one significantly influence the cytotoxic activity. The above SARs also suggest that prospective antitumor agents with better cytotoxic activity may be obtained from a good combination of the substituents at C5-position of the indolin-2-one ring and the side chain at 4'-position of the benzylidene ring. Based on the promising cytotoxic activity, most active compound **4p** from this series was taken-up for further mechanism of cell growth inhibition and cell-cycle arrest studies.

<insert Table 1 here>

2.2.2. Morphology

To examine whether the treatment with the compound could lead to loss of cell viability and induction of apoptosis, PC-3 cells were treated with different concentrations of the most potent compound **4p** for 48 h. Cells were observed and photographs were taken under a phase contrast microscope (Nikon). It can be inferred from the **Figure 3** that the treatment with compound **4p** resulted in markedly decreased number of viable cells of prostate PC-3 cancer cells in comparison to the vehicle treated control cells as observed by the distinctive morphological features of cells including detachment and cell shrinkage. Moreover, the percentages of viable cells were determined after treatment with increasing concentrations (1, 2 and 4 μM) of compound **4p** by using trypan blue assay. It was observed that at concentrations of 2 or 4 μM , compound **4p** displayed significant cytotoxicity (53% and 45% viable cells, respectively) in PC-3 cells as shown in **Figure 3**.

<insert Figure 3 here>

2.2.3. *In vitro* cell migration assay

Wound healing assay was carried out to investigate the effect of compound **4p** on migration potential of PC-3 cells [36]. Wounds were created in the monolayer cultures of PC-3 cells with a 200 μ L pipette tip and cells were allowed to migrate into the wound area for 0, 24, and 48 h. The migration of prostate cancer cells to fill-up the 'wound' was recorded by microscopic observations. As shown in **Figure 4**, after 24 h the untreated control cells had filled 43.4% in the scratched area, whereas compound **4p** treatment resulted in inhibition of cell migration with 37.3%, 29.4% and 7.3% cells migrated in the wounded area with the doses of 1, 2, and 4 μ M, respectively. The effect was more prominent with 1 and 2 μ M doses after 48 h. It can be inferred from the results that the compound **4p** suppresses the migration potential of the prostate cancer cells in dose dependent manner and also causes a significant reduction in cell number, which can be induced by cytostatic, or even cytotoxic activity at the concentrations used.

<Insert Figure 4 here>

2.2.4. Effect on Structures of F-actin

Previous reports suggested that a migration of cells depends on the formation of membrane protrusions in response to chemotactic stimuli [37]. The driving force for the formation of membrane protrusion is localized actin filaments polymerization which leads to stress fibre assembly and plays a crucial role in cell motility. As **4p** inhibits the migration of prostate cancer cells, it was of interest to investigate the effect on stress fibre formation. The formation of the actin cytoskeleton in PC-3 cells was established by rhodamine-phalloidin staining which is red fluorescent dye that specifically binds to F-actin and images were

captured with confocal microscope. As shown in **Figure 5**, control cells exhibited a large number of F-actin extensions and stress fibre formation at the periphery of the cells, whereas compound treated cells displayed disrupted stress fibres around the nucleus and the numbers were decreased. Collectively, these results demonstrated that the compound **4p** inhibit the migration of prostate cancer cells through disruption of actin formation.

<insert Figure 5 here>

2.2.5. Cell cycle analysis

In order to further investigate the mechanism of cell growth inhibition of compound **4p**, cell cycle analysis on PC-3 cells was carried out using propidium iodide staining [38]. PC-3 cells were treated with different concentrations (1, 2, and 4 μM) of compound **4p** for 24 h and cell cycle distribution was observed by flow-cytometric analysis after staining with propidium iodide. As shown in **Figure 6**, the treatment with compound **4p** resulted in significant increase in ratio of PC-3 cells in G2/M phase from 19.2% to 55.7% when compared to the control cells with a concomitant decrease in the number of cells at G0/G1 phase in a dose dependent manner. The G2/M phase content was more prominent at 4 μM concentration which indicates that the compound **4p** arrested the PC-3 cells in G2/M phase.

<insert Figure 6 here>

2.2.6. Apoptosis detection studies

The ability of tumor cells to evade apoptosis, or programmed cell death, is a hallmark of human cancers [39]. In addition to cancer cell survival, defects in apoptotic pathways may also contribute to tumor progression and chemo-resistance. Thus, inducing apoptosis in cancer cells has emerged as an attractive strategy in cancer therapy. Therefore, it was

considered of interest to investigate the apoptosis inducing effect of compound **4p** on PC-3 cells.

2.2.6.1. Hoechst staining

The morphological changes induced by the compound **4p** in prostate cancer cells were investigated using Hoechst nuclear staining [40]. PC-3 cells were treated with the various concentrations of the compound **4p** (1, 2 and 4 μ M) for 24 h and stained with Hoechst 33242. The results from the **Figure 7** demonstrates that the compound **4p** treated cells displayed typical apoptotic characteristics such as chromatin condensation (brightly stained cells as indicated by arrows) and nuclear fragmentation in a concentration dependent manner, whereas vehicle treated (DMSO) control cells showed an even distribution of staining of homogeneous nuclei. These results indicated that the compound **4p** could induce apoptosis in PC-3 cells.

<insert Figure 7 here>

2.2.6.2. Effect of compound **4p** on mitochondrial membrane potential ($D\Psi_m$)

Studies showed that the mitochondria also play a critical role in the intrinsic pathway of apoptosis as they are the key targets of cellular oxidative stress, which hampers the electron transport chain, leading to reactive oxygen species (ROS) generation and depolarization of $D\Psi_m$ [41]. Therefore, to assess the influence of compound **4p** on mitochondria, the $D\Psi_m$ was measured. Treatment of prostate cancer PC-3 cells with compound **4p** caused 19–42% decrease in $D\Psi_m$ compared to control cells (**Fig. 8**). The compound **4p** dose-dependently induced dissipation of $D\Psi_m$. At 4 μ M, the compound **4p** was found to be more potent in dissipating $D\Psi_m$ which induces 42% loss compared to the control which is indicative of the lethal effects on mitochondria, thereby promoting the ensuing events of apoptosis.

<insert Figure 8 here>

2.2.6.3. Effect of compound **4p** on intracellular Ca^{2+} levels

Previous reports suggested that elevated levels of intracellular Ca^{2+} is one of the major contributing factors towards the changes in mitochondrial membrane potential $\Delta\Psi_m$ [42]. Therefore, the effect of compound **4p** on intracellular Ca^{2+} was investigated to further confirm its role in inducing $\Delta\Psi_m$ depolarization. The results from the **Figure 9** indicated that the compound treatment caused increase in the intracellular calcium levels in a dose dependent manner compared to control in PC-3 cells. At 2 μM , there was a significant increase in Ca^{2+} levels compared to control and at 4 μM it was found to be more potent in increasing Ca^{2+} .

<insert Figure 9 here>

2.2.6.4. AnnexinV-FITC/Propidium iodide dual staining assay

To quantify the percentage of apoptosis induced by compound **4p**, the Annexin V-FITC/Propidium iodide dual staining assay [43] was carried out using prostate PC-3 cancer cells. The Annexin V-FITC/PI dual staining assay facilitates the detection of live cells (Q1-LL; AV-/PI-), early apoptotic cells (Q1-LR; AV+/PI-), late apoptotic cells (Q1-UR-AV+/PI+) and necrotic cells (Q1-UL; AV-/PI+). As shown in **Figure 10**, the percentage of total apoptotic cells (early and late apoptotic cells) was increased to 38.2% after treatment with 4 μM concentration of compound **4p** for 24 h, in comparison to the control (9.4%) cells. The percentage of early and late apoptotic cells were significantly increased with increase in concentrations of the compound **4p**, which indicates that the compound **4p** induces apoptosis in PC-3 cells in a dose dependent manner.

<insert Figure 10 here>

2.2.7. Western blotting

Caspases play an important role in the apoptosis process. Particularly, the caspase-3 is a frequently activated death protease which catalyzes the specific cleavage of many key cellular proteins [44]. We examined the effect of compound **4p** on the activation of caspase-3 by western blotting. As shown in **Figure 11**, compound **4p** dose dependently increased the activation of caspase-3. Subsequently, we demonstrated the effect of compound **4p** on Bcl2 family proteins. Apoptosis is associated with changes in the expression of anti-apoptotic protein Bcl-2 and pro-apoptotic protein Bax [45]. We observed that compound **4p** dose dependently decreased the Bcl2 expression and increased the Bax expression. These results show that compound **4p** induces apoptosis through activation of caspase-3 and up-regulation of pro-apoptotic Bax and down regulation of anti-apoptotic Bcl-2 proteins.

<insert Figure 11 here>

3.0. Conclusion

In conclusion, we have designed and synthesized a series of (Z)-3-(3'-methoxy-4'-(2-amino-2-oxoethoxy)-benzylidene)indolin-2-one derivatives and evaluated for their antiproliferative activity against selected human cancer cell lines. Among them, one of the compounds **4p** displayed potent growth inhibition on PC-3 cells. The exposure of prostate PC-3 cancer cells to the compound **4p** resulted in a remarkable inhibition of *in vitro* cell migration through disorganization and disruption of F-actin structures. Flow cytometry analysis indicated that the compound **4p** arrested the cells at G2/M phase of the cell cycle. The apoptosis inducing effect of the compound was analyzed by Hoechst nuclear staining. Moreover, the compound **4p** induces apoptosis in PC-3 cells through collapse of mitochondrial membrane potential and elevation of intracellular Ca²⁺ levels. Western blotting analysis demonstrated that compound **4p** induces apoptosis through activation of caspase-3 and up-regulation of pro-apoptotic Bax

and down regulation of anti-apoptotic Bcl-2 proteins. Overall, the simple synthetic preparation and their biological properties make these derivatives as promising new chemical entities for the development of cancer therapeutics.

4.0. Materials & Methods

4.1. Chemistry

All the starting materials and other reagents were commercially available of the best grade and were used without further purification; substituted anilines, vanillin, piperidine, morpholine, pyrrolidine, piperidine, dimethylmorpholine, indoline and chloro-acetyl chloride (Spectrochem); chloral hydrate, $\text{NH}_2\text{OH}\cdot\text{HCl}$ and $\text{NH}_2\text{NH}_2\cdot\text{H}_2\text{O}$ (Aldrich); and ethylene glycol, DMF and acetonitrile (Finar Chemicals). The progress of the reactions were monitored by thin layer chromatography (TLC), performed on MERCK pre-coated silica gel 60-F₂₅₄ aluminum plates. Spots were visualized by UV light. All melting points were recorded on Stuart[®] SMP30 melting point apparatus and are uncorrected. ¹H and ¹³C NMR spectra were recorded on Bruker Avance 500 MHz spectrometer and referenced to residual solvents. Chemical shifts are reported in parts per million (ppm) and referenced to residual DMSO-*d*₆ (δ 2.50) (for ¹H spectra) or DMSO-*d*₆ (δ 39.52) (for ¹³C spectra). Spin multiplicities are described as s (singlet), brs (broad singlet), d (doublet), dd (double doublet), t (triplet), q (quartet), or m (multiplet). Coupling constants are reported in hertz (Hz). HRMS analyses were acquired on Agilent Q-TOF-Mass Spectrometer 6540-UHD and carried out in the ESI techniques at 70 eV.

4.1.1. General procedure for synthesis of oxindoles (7a-e)

To a mixture of isatin (**6a-e**, 1.0 g) and hydrazine-hydrate (5 mL, ~30 mmol) in ethylene glycol, potassium hydroxide (10 equiv.) was added and the resulting reaction mixture was

stirred at 110–130 °C for 2–3 h (reaction monitored by TLC). The reaction mixture was cooled to room temperature, poured into ice-cold water (50 mL), acidified to pH 2 with 6N hydrochloric acid and extracted with ethyl acetate (3 x 30 mL). The organic extracts were combined, washed with brine (15 mL), dried over sodium sulfate and concentrated *in vacuo*. The obtained residue was purified by column chromatography using ethyl acetate–hexane as eluents to furnish **7a–e** in moderate yields.

4.1.2. General procedure for the synthesis of (Z)-3-(3'-methoxy-4'-(2-amino-2-oxoethoxy)-benzylidene)indolin-2-one derivatives (**4a–v**)

To a solution of appropriate oxindole (**7a–e**, 0.3 mmol) in ethanol (3 mL) was added corresponding aldehydes (**11a–e**, 0.32 mmol) and a catalytic amount of piperidine. The reaction mixture was stirred at reflux for 6–12 h (reaction monitored by TLC). After cooling, the precipitate was filtered, washed with cold ethanol, and dried in air to furnish pure (Z)-3-(3'-methoxy-4'-(2-amino-2-oxoethoxy)-benzylidene)indolin-2-ones title compounds of formula (**4a–v**) as yellow/brown/orange solids in moderate to excellent yields.

4.1.2.1. (Z)-3-(3'-Methoxy-4'-(2-morpholino-2-oxoethoxy)benzylidene)indolin-2-one (**4a**). Yellow solid, yield 85%; Mp: 234–236 °C; ¹H NMR (500 MHz, DMSO-*d*₆): δ 3.43–3.51 (m, 4H), 3.55–3.65 (m, 4H), 3.86 (s, 3H), 4.94 (s, 2H), 6.83 (d, *J* = 7.6 Hz, 1H), 6.98 (t, *J* = 8.7 Hz, 2H), 7.18 (t, *J* = 7.7 Hz, 1H), 7.67 (d, *J* = 7.5 Hz, 1H), 7.74 (s, 1H), 7.81 (dd, *J* = 1.6, 8.6 Hz, 1H), 8.64 (d, *J* = 1.6 Hz, 1H), 10.56 (s, 1H); ¹³C NMR (125 MHz, DMSO-*d*₆): δ 41.6, 44.8, 55.5, 66.0, 66.1, 66.2, 109.2, 112.5, 115.4, 119.2, 120.9, 124.1, 125.4, 126.9, 127.6, 128.2, 137.2, 140.2, 148.0, 149.2, 165.6, 167.4; HRMS (ESI): *m/z* calcd. for C₂₂H₂₃N₂O₅, 395.1607, found 395.1596 [M+H]⁺.

4.1.2.2. (Z)-5-Fluoro-3-(3'-methoxy-4'-(2-morpholino-2-oxoethoxy)benzylidene)indolin-2-one (**4b**). Yellow solid, yield 83%; Mp: 259–261 °C; ¹H NMR (500 MHz, DMSO-*d*₆): δ 3.44–

3.50 (m, 4H), 3.55–3.64 (m, 4H), 3.86 (s, 3H), 4.95 (s, 2H), 6.77–6.83 (m, 1H), 6.96–7.03 (m, 2H), 7.60 (dd, $J = 2.4, 9.0$ Hz, 1H), 7.78–7.86 (m, 2H), 8.66 (d, $J = 1.6$ Hz, 1H), 10.57 (s, 1H); ^{13}C NMR (125 MHz, DMSO- d_6): δ 41.6, 44.7, 55.5, 65.9, 66.0, 66.1, 106.6 (d, $J_{CF} = 25.2$ Hz), 109.9, (d, $J_{CF} = 8.1$ Hz), 112.5, 114.3 (d, $J_{CF} = 23.7$ Hz), 115.5, 123.7 (d, $J_{CF} = 2.5$ Hz), 126.9 (d, $J_{CF} = 8.8$ Hz), 127.3, 127.4, 136.4, 139.0, 148.0, 150.1, 157.9 (d, $J_{CF} = 233.2$ Hz), 165.6, 167.4; HRMS (ESI): m/z calcd. for $\text{C}_{22}\text{H}_{22}\text{FN}_2\text{O}_5$, 413.1513, found 413.1514 $[\text{M}+\text{H}]^+$.

4.1.2.3. (*Z*)-5-Chloro-3-(3'-methoxy-4'-(2-morpholino-2-oxoethoxy)benzylidene)indolin-2-one (**4c**). Yellow solid, yield 87%; Mp: 253–254 °C; ^1H NMR (500 MHz, DMSO- d_6): δ 3.43–3.50 (m, 4H), 3.55–3.65 (m, 4H), 3.85 (s, 3H), 4.95 (s, 2H), 6.83 (d, $J = 8.2$ Hz, 1H), 6.98 (d, $J = 8.5$ Hz, 1H), 7.20 (dd, $J = 2.1, 8.2$ Hz, 1H), 7.80 (d, $J = 2.0$ Hz, 1H), 7.84 (dd, $J = 1.8, 8.6$ Hz, 1H), 7.88 (s, 1H), 8.65 (d, $J = 1.9$ Hz, 1H), 10.68 (s, 1H); ^{13}C NMR (125 MHz, DMSO- d_6): δ 41.6, 44.7, 55.6, 65.9, 66.0, 66.1, 110.5, 112.5, 115.5, 119.2, 122.9, 125.3, 127.3, 127.4 (2C), 127.5, 138.8, 139.3, 148.0, 150.2, 165.5, 167.2; HRMS (ESI): m/z calcd. for $\text{C}_{22}\text{H}_{22}\text{ClN}_2\text{O}_5$, 429.1217, found 429.1211 $[\text{M}+\text{H}]^+$.

4.1.2.4. (*Z*)-5-Bromo-3-(3'-methoxy-4'-(2-morpholino-2-oxoethoxy)benzylidene)indolin-2-one (**4d**). Yellow solid, yield 82%; Mp: 246–248 °C; ^1H NMR (500 MHz, DMSO- d_6): δ 3.43–3.51 (m, 4H), 3.55–3.65 (m, 4H), 3.85 (s, 3H), 4.95 (s, 2H), 6.79 (d, $J = 8.2$ Hz, 1H), 6.99 (d, $J = 8.5$ Hz, 1H), 7.20 (dd, $J = 1.9, 8.2$ Hz, 1H), 7.85 (dd, $J = 1.8, 8.6$ Hz, 1H), 7.88 (s, 1H), 7.93 (d, $J = 1.9$ Hz, 1H), 8.65 (d, $J = 1.6$ Hz, 1H), 10.69 (s, 1H); ^{13}C NMR (125 MHz, DMSO- d_6): δ 41.6, 44.7, 55.5, 65.9, 66.0, 66.1, 111.0, 112.5, 113.0, 115.5, 121.9, 122.8, 127.4 (2C), 127.8, 130.3, 139.1, 139.3, 148.0, 150.2, 165.5, 167.0; HRMS (ESI): m/z calcd. for $\text{C}_{22}\text{H}_{22}\text{BrN}_2\text{O}_5$, 473.0712, found 473.0673 $[\text{M}+\text{H}]^+$.

4.1.2.5. (Z)-3-(3'-Methoxy-4'-(2-morpholino-2-oxoethoxy)benzylidene)-5-methylindolin-2-one (**4e**). Orange solid, yield 91%; Mp: 214–216 °C; ¹H NMR (500 MHz, DMSO-*d*₆): δ 2.30 (s, 3H), 3.43–3.50 (m, 4H), 3.55–3.64 (m, 4H), 3.85 (s, 3H), 4.93 (s, 2H), 6.71 (d, *J* = 7.8 Hz, 1H), 6.96 (d, *J* = 8.5 Hz, 1H), 6.99 (d, *J* = 7.8 Hz, 1H), 7.50 (s, 1H), 7.70 (s, 1H), 7.81 (dd, *J* = 1.7, 8.5 Hz, 1H), 8.65 (d, *J* = 1.7 Hz, 1H), 10.44 (s, 1H); ¹³C NMR (125 MHz, DMSO-*d*₆): δ 20.8, 41.6, 44.8, 55.5, 66.0, 66.1, 66.2, 108.9, 112.5, 115.4, 119.7, 124.3, 125.4, 126.8, 127.7, 128.6, 129.6, 137.9, 138.0, 148.0, 149.6, 165.6, 167.5; HRMS (ESI): *m/z* calcd. for C₂₃H₂₅N₂O₅, 409.1763, found 409.1800 [M+H]⁺.

4.1.2.6. (Z)-3-(3'-Methoxy-4'-(2-oxo-2-(piperidin-1-yl)ethoxy)benzylidene)indolin-2-one (**4f**). Yellow solid, yield 84%; Mp: 212–214 °C; ¹H NMR (500 MHz, DMSO-*d*₆): δ 1.36–1.65 (m, 6H), 3.39–3.47 (m, 4H), 3.85 (s, 3H), 4.90 (s, 2H), 6.83 (d, *J* = 7.6 Hz, 1H), 6.94 (d, *J* = 8.5 Hz, 1H), 6.98 (t, *J* = 7.6 Hz, 1H), 7.18 (t, *J* = 7.7 Hz, 1H), 7.67 (d, *J* = 7.4 Hz, 1H), 7.74 (s, 1H), 7.80 (dd, *J* = 1.8, 8.5 Hz, 1H), 8.65 (d, *J* = 1.8 Hz, 1H), 10.56 (s, 1H); ¹³C NMR (125 MHz, DMSO-*d*₆): δ 23.9, 25.2, 25.9, 42.2, 45.2, 55.5, 66.4, 109.2, 112.3, 115.4, 119.2, 120.9, 124.1, 125.4, 126.9, 127.5, 128.2, 137.2, 140.2, 148.0, 149.8, 165.0, 167.4; HRMS (ESI): *m/z* calcd. for C₂₃H₂₅N₂O₄, 393.1814, found 393.1838 [M+H]⁺.

4.1.2.7. (Z)-5-Fluoro-3-(3'-methoxy-4'-(2-oxo-2-(piperidin-1-yl)ethoxy)benzylidene)indolin-2-one (**4g**). Yellow solid, yield 84%; Mp: 221–223 °C; ¹H NMR (500 MHz, DMSO-*d*₆): δ 1.40–1.63 (m, 6H), 3.38–3.46 (m, 4H), 3.85 (s, 3H), 4.91 (s, 2H), 6.78–6.82 (m, 1H), 6.96 (d, *J* = 8.5 Hz, 1H), 7.00 (dt, *J* = 2.6, 9.5 Hz, 1H), 7.60 (dd, *J* = 2.5, 9.1 Hz, 1H), 7.80 (dd, *J* = 1.8, 8.6 Hz, 1H), 7.82 (s, 1H), 8.67 (d, *J* = 1.9 Hz, 1H), 10.57 (s, 1H); ¹³C NMR (125 MHz, DMSO-*d*₆): δ 23.9, 25.3, 25.9, 42.2, 45.2, 55.5, 66.4, 106.6 (d, *J*_{CF} = 25.3 Hz), 109.9 (d, *J*_{CF} = 8.3 Hz), 112.4, 114.3 (d, *J*_{CF} = 23.7 Hz), 115.5, 123.7 (d, *J*_{CF} = 2.4 Hz), 127.0 (d, *J*_{CF} = 8.7 Hz), 127.3, 127.4, 136.4, 139.0, 148.0, 150.3, 157.9 (d, *J*_{CF} = 233.3 Hz), 165.0, 167.5; HRMS (ESI): *m/z* calcd. for C₂₃H₂₄FN₂O₄, 411.1720, found 411.1690 [M+H]⁺.

4.1.2.8. (Z)-5-Chloro-3-(3'-methoxy-4'-(2-oxo-2-(piperidin-1-yl)ethoxy)benzylidene)indolin-2-one (**4h**). Yellow solid, yield 87%; Mp: 230–232 °C; ¹H NMR (500 MHz, DMSO-*d*₆): δ 1.41–1.63 (m, 6H), 3.38–3.46 (m, 4H), 3.85 (s, 3H), 4.91 (s, 2H), 6.83 (d, *J* = 8.2 Hz, 1H), 6.96 (d, *J* = 8.5 Hz, 1H), 7.21 (dd, *J* = 2.0, 8.2 Hz, 1H), 7.81 (d, *J* = 2.0 Hz, 1H), 7.83 (dd, *J* = 1.8, 8.6 Hz, 1H), 7.88 (s, 1H), 8.66 (d, *J* = 1.8 Hz, 1H), 10.68 (s, 1H); ¹³C NMR (125 MHz, DMSO-*d*₆): δ 23.9, 25.3, 25.9, 42.2, 45.2, 55.5, 66.3, 110.6, 112.4, 115.5, 119.2, 122.9, 125.3, 127.3, 127.4, 127.5 (2C), 138.8, 139.3, 148.0, 150.3, 165.0, 167.2; HRMS (ESI): *m/z* calcd. for C₂₃H₂₄ClN₂O₄, 427.1425, found 427.1461 [M+H]⁺.

4.1.2.9. (Z)-5-Bromo-3-(3'-methoxy-4'-(2-oxo-2-(piperidin-1-yl)ethoxy)benzylidene)indolin-2-one (**4i**). Orange solid, yield 83%; Mp: 224–225 °C; ¹H NMR (500 MHz, DMSO-*d*₆): δ 1.40–1.62 (m, 6H), 3.39–3.46 (m, 4H), 3.85 (s, 3H), 4.91 (s, 2H), 6.78 (d, *J* = 8.2 Hz, 1H), 6.96 (d, *J* = 8.5 Hz, 1H), 7.33 (d, *J* = 8.2 Hz, 1H), 7.84 (dd, *J* = 1.8, 8.5 Hz, 1H), 7.88 (s, 1H), 7.93 (s, 1H), 8.65 (d, *J* = 1.7 Hz, 1H), 10.69 (s, 1H); ¹³C NMR (125 MHz, DMSO-*d*₆): δ 23.9, 25.3, 25.9, 42.2, 45.2, 55.5, 66.3, 111.1, 112.4, 113.0, 115.5, 122.0, 122.7, 127.3, 127.5, 127.8, 130.3, 139.2, 139.3, 148.0, 150.3, 165.0, 167.1; HRMS (ESI): *m/z* calcd. for C₂₃H₂₄BrN₂O₄, 473.0899, found 473.0922 [M+H]⁺.

4.1.2.10. (Z)-3-(3'-Methoxy-4'-(2-oxo-2-(piperidin-1-yl)ethoxy)benzylidene)-5-methylindolin-2-one (**4j**). Orange crystalline solid, yield 89%; Mp: 213–214 °C; ¹H NMR (500 MHz, DMSO-*d*₆): δ 1.40–1.61 (m, 6H), 2.30 (s, 3H), 3.39–3.45 (m, 4H), 3.85 (s, 3H), 4.89 (s, 2H), 6.72 (d, *J* = 7.8 Hz, 1H), 6.94 (d, *J* = 8.5 Hz, 1H), 6.99 (d, *J* = 7.8 Hz, 1H), 7.50 (s, 1H), 7.70 (s, 1H), 7.80 (d, *J* = 8.3 Hz, 1H), 8.66 (s, 1H), 10.45 (s, 1H); ¹³C NMR (125 MHz, DMSO-*d*₆): δ 20.8, 23.9, 25.3, 25.9, 42.2, 45.2, 55.5, 66.4, 108.9, 112.3, 115.3, 119.7, 124.2, 125.4, 126.9, 127.6, 128.6, 129.6, 136.9, 138.0, 148.0, 149.8, 165.0, 167.5; HRMS (ESI): *m/z* calcd. for C₂₄H₂₇N₂O₄, 407.1971, found 407.1968 [M+H]⁺.

4.1.2.11. (Z)-3-(3'-Methoxy-4'-(2-oxo-2-(pyrrolidin-1-yl)ethoxy)benzylidene)indolin-2-one (**4k**). Yellow solid, yield 86%; Mp: 210–212 °C; ¹H NMR (500 MHz, DMSO-*d*₆): δ 1.74–1.82 (m, 2H), 1.86–1.94 (m, 2H), 3.30–3.36 (m, 2H), 3.48 (t, *J* = 6.8 Hz, 2H), 3.85 (s, 3H), 4.82 (s, 2H), 6.83 (d, *J* = 7.6 Hz, 1H), 6.94 (d, *J* = 8.5 Hz, 1H), 6.98 (t, *J* = 7.6 Hz, 1H), 7.18 (t, *J* = 7.7 Hz, 1H), 7.67 (d, *J* = 7.5 Hz, 1H), 7.74 (s, 1H), 7.81 (dd, *J* = 1.7, 8.6 Hz, 1H), 8.64 (d, *J* = 1.8 Hz, 1H), 10.56 (s, 1H); ¹³C NMR (125 MHz, DMSO-*d*₆): δ 23.5, 25.7, 44.7, 45.6, 55.5, 66.5, 109.2, 112.4, 115.3, 119.2, 120.9, 124.0, 125.4, 126.9, 127.5, 128.2, 137.3, 140.2, 148.0, 149.9, 165.2, 167.4; HRMS (ESI): *m/z* calcd. for C₂₂H₂₃N₂O₄, 379.1658, found 379.1631 [M+H]⁺.

4.1.2.12. (Z)-5-Fluoro-3-(3'-methoxy-4'-(2-oxo-2-(pyrrolidin-1-yl)ethoxy)benzylidene)indolin-2-one (**4l**). Orange solid, yield 85%; Mp: 244–246 °C; ¹H NMR (500 MHz, DMSO-*d*₆): δ 1.75–1.81 (m, 2H), 1.87–1.94 (m, 2H), 3.29–3.35 (m, 2H), 3.48 (t, *J* = 6.8 Hz, 2H), 3.85 (s, 3H), 4.83 (s, 2H), 6.76–6.82 (m, 1H), 6.96 (d, *J* = 8.5 Hz, 1H), 7.00 (dt, *J* = 2.6, 8.6 Hz, 1H), 7.60 (dd, *J* = 2.5, 9.1 Hz, 1H), 7.80 (dd, *J* = 1.8, 8.6 Hz, 1H), 7.82 (s, 1H), 8.66 (d, *J* = 1.9 Hz, 1H), 10.57 (s, 1H); ¹³C NMR (125 MHz, DMSO-*d*₆): δ 23.5, 25.7, 44.7, 45.6, 55.5, 66.4, 106.6 (d, *J*_{CF} = 25.2 Hz), 109.9 (d, *J*_{CF} = 8.3 Hz), 112.4, 114.3 (d, *J*_{CF} = 23.8 Hz), 115.4, 123.7 (d, *J*_{CF} = 2.4 Hz), 127.0 (d, *J*_{CF} = 8.9 Hz), 127.3, 127.4, 136.4, 139.1, 148.0, 150.3, 157.9 (d, *J*_{CF} = 233.3 Hz), 165.2, 167.5; HRMS (ESI): *m/z* calcd. for C₂₂H₂₂FN₂O₄, 397.1564, found 379.1580 [M+H]⁺.

4.1.2.13. (Z)-5-Chloro-3-(3'-methoxy-4'-(2-oxo-2-(pyrrolidin-1-yl)ethoxy)benzylidene)indolin-2-one (**4m**). Yellow solid, yield 88%; Mp: 246–247 °C; ¹H NMR (500 MHz, DMSO-*d*₆): δ 1.74–1.80 (m, 2H), 1.86–1.92 (m, 2H), 3.27–3.34 (m, 2H), 3.47 (t, *J* = 6.8 Hz, 2H), 3.85 (s, 3H), 4.82 (s, 2H), 6.82 (d, *J* = 8.2 Hz, 1H), 6.94 (d, *J* = 8.5 Hz, 1H), 7.19 (dd, *J* = 2.1, 8.2 Hz, 1H), 7.79 (d, *J* = 2.0 Hz, 1H), 7.82 (dd, *J* = 1.8, 8.6 Hz, 1H), 7.86 (s, 1H), 8.64 (d, *J* = 1.9 Hz, 1H), 10.67 (s, 1H); ¹³C NMR (125 MHz, DMSO-*d*₆): δ

23.5, 25.6, 44.7, 45.6, 55.4, 66.4, 110.5, 112.4, 115.4, 119.2, 122.8, 125.3, 127.3, 127.4, 127.5 (2C), 138.8, 139.2, 147.9, 150.3, 165.1, 167.2; HRMS (ESI): m/z calcd. for $C_{22}H_{22}ClN_2O_4$, 413.1268, found 413.1234 $[M+H]^+$.

4.1.2.14. *(Z)*-5-Bromo-3-(3'-methoxy-4'-(2-oxo-2-(pyrrolidin-1-yl)ethoxy)benzylidene)indolin-2-one (**4n**). Brown solid, yield 85%; Mp: 221–223 °C; 1H NMR (500 MHz, DMSO- d_6): δ 1.74–1.80 (m, 2H), 1.86–1.92 (m, 2H), 3.30–3.34 (m, 2H), 3.47 (t, $J = 6.8$ Hz, 2H), 3.84 (s, 3H), 4.82 (s, 2H), 6.77 (d, $J = 8.2$ Hz, 1H), 6.95 (d, $J = 8.5$ Hz, 1H), 7.32 (dd, $J = 1.9, 8.2$ Hz, 1H), 7.83 (dd, $J = 1.8, 8.6$ Hz, 1H), 7.87 (s, 1H), 7.91 (d, $J = 1.8$ Hz, 1H), 8.64 (d, $J = 1.8$ Hz, 1H), 10.68 (s, 1H); ^{13}C NMR (125 MHz, DMSO- d_6): δ 23.5, 25.6, 44.7, 45.6, 55.4, 66.4, 111.0, 112.4, 112.9, 115.5, 121.9, 122.7, 127.3, 127.5, 127.8, 130.2, 139.1, 139.3, 147.9, 150.3, 165.1, 167.0; HRMS (ESI): m/z calcd. for $C_{22}H_{22}BrN_2O_4$, 459.0742, found 459.0741 $[M+H]^+$.

4.1.2.15. *(Z)*-3-(3'-Methoxy-4'-(2-oxo-2-(pyrrolidin-1-yl)ethoxy)benzylidene)-5-methylindolin-2-one (**4o**). Orange solid, yield 88%; Mp: 226–228 °C; 1H NMR (500 MHz, DMSO- d_6): δ 1.74–1.80 (m, 2H), 1.86–1.92 (m, 2H), 2.29 (s, 3H), 3.29–3.34 (m, 2H), 3.47 (t, $J = 6.8$ Hz, 2H), 3.84 (s, 3H), 4.80 (s, 2H), 6.70 (d, $J = 7.8$ Hz, 1H), 6.93 (d, $J = 8.5$ Hz, 1H), 6.98 (d, $J = 7.8$ Hz, 1H), 7.49 (s, 1H), 7.68 (s, 1H), 7.80 (dd, $J = 1.7, 8.5$ Hz, 1H), 8.64 (d, $J = 1.6$ Hz, 1H), 10.43 (s, 1H); ^{13}C NMR (125 MHz, DMSO- d_6): δ 20.8, 23.5, 25.6, 44.7, 45.6, 55.4, 66.4, 108.9, 112.4, 115.3, 119.7, 124.2, 125.4, 126.9, 127.6, 128.6, 129.6, 136.9, 138.0, 147.9, 149.8, 165.2, 167.5; HRMS (ESI): m/z calcd. for $C_{23}H_{25}N_2O_4$, 393.1814, found 393.1812 $[M+H]^+$.

4.1.2.16. *(Z)*-3-(4'-(2-(Indolin-1-yl)-2-oxoethoxy)-3'-methoxybenzylidene)indolin-2-one (**4p**). Yellow solid, yield 89%; Mp: 239–241 °C; 1H NMR (500 MHz, DMSO- d_6): δ 3.20 (t, $J = 8.3$ Hz, 2H), 3.88 (s, 3H), 4.18 (t, $J = 8.4$ Hz, 2H), 5.04 (s, 2H), 6.83 (d, $J = 7.6$ Hz, 1H), 6.95–

7.07 (m, 3H), 7.13–7.20 (m, 2H), 7.27 (d, $J = 7.3$ Hz, 1H), 7.67 (d, $J = 7.5$ Hz, 1H), 7.75 (s, 1H), 7.81 (d, $J = 8.5$ Hz, 1H), 8.02 (d, $J = 8.0$ Hz, 1H), 8.68 (d, $J = 1.9$ Hz, 1H), 10.57 (s, 1H); ^{13}C NMR (125 MHz, DMSO- d_6): δ 27.7, 45.8, 55.5, 66.3, 109.2, 112.5, 115.4, 115.8, 119.2, 120.9, 123.6, 124.1, 124.9, 125.4, 126.9, 127.1, 127.6, 128.2, 131.5, 137.3, 140.2, 142.7, 147.9, 149.8, 165.4, 167.4; HRMS (ESI): m/z calcd. for $\text{C}_{26}\text{H}_{23}\text{N}_2\text{O}_4$, 427.1658, found 427.1651 $[\text{M}+\text{H}]^+$.

4.1.2.17. (*Z*)-3-(4'-(2-(Indolin-1-yl)-2-oxoethoxy)-3'-methoxybenzylidene)-5-methylindolin-2-one (**4q**). Orange solid, yield 91%; Mp: 244–246 °C; ^1H NMR (500 MHz, DMSO- d_6): δ 2.30 (s, 3H), 3.20 (t, $J = 8.0$ Hz, 2H), 3.88 (s, 3H), 4.18 (t, $J = 8.2$ Hz, 2H), 5.04 (s, 2H), 6.72 (d, $J = 7.7$ Hz, 1H), 6.94–7.10 (m, 3H), 7.16 (t, $J = 7.6$ Hz, 1H), 7.27 (d, $J = 7.1$ Hz, 1H), 7.50 (s, 1H), 7.71 (s, 1H), 7.81 (d, $J = 7.8$ Hz, 1H), 8.02 (d, $J = 7.8$ Hz, 1H), 8.69 (s, 1H), 10.44 (s, 1H); ^{13}C NMR (125 MHz, DMSO- d_6): δ 20.8, 27.7, 45.8, 55.5, 66.3, 108.9, 112.5, 115.4, 115.8, 119.7, 123.6, 124.3, 124.9, 125.5, 126.9, 127.0, 127.7, 128.6, 129.6, 131.5, 136.9, 138.0, 142.7, 147.9, 149.7, 165.4, 167.5; HRMS (ESI): m/z calcd. for $\text{C}_{27}\text{H}_{25}\text{N}_2\text{O}_4$, 441.1814, found 441.1816 $[\text{M}+\text{H}]^+$.

4.1.2.18. (*Z*)-3-(4'-(2-(2,6-Dimethylmorpholino)-2-oxoethoxy)-3'-methoxybenzylidene)indolin-2-one (**4r**). Yellow solid, yield 85%; Mp: 233–234 °C; ^1H NMR (500 MHz, DMSO- d_6): δ 1.09 (d, $J = 6.2$ Hz, 3H), 1.09 (d, $J = 6.2$ Hz, 3H), 2.30 (t, $J = 12.5$ Hz, 1H), 2.73 (t, $J = 10.7$ Hz, 1H), 3.38–3.48 (m, 1H), 3.51–3.60 (m, 1H), 3.78 (d, $J = 13.0$ Hz, 1H), 3.85 (s, 3H), 4.18 (d, $J = 12.9$ Hz, 1H), 4.87 (d, $J = 14.7$ Hz, 1H), 5.00 (d, $J = 14.7$ Hz, 1H), 6.83 (d, $J = 7.6$ Hz, 1H), 6.94–7.02 (m, 2H), 7.18 (dt, $J = 1.0, 7.6$ Hz, 1H), 7.67 (d, $J = 7.5$ Hz, 1H), 7.74 (s, 1H), 7.81 (dd, $J = 1.9, 8.6$ Hz, 1H), 8.65 (d, $J = 1.9$ Hz, 1H), 10.56 (s, 1H); ^{13}C NMR (125 MHz, DMSO- d_6): δ 18.3, 18.6, 46.6, 49.7, 55.5, 66.2, 71.1, 71.3, 109.2, 112.5, 115.3, 119.2, 120.9, 124.1, 125.4, 126.9, 127.6, 128.2, 137.2, 140.2, 148.0, 149.7, 165.3, 167.4; HRMS (ESI): m/z calcd. for $\text{C}_{24}\text{H}_{27}\text{N}_2\text{O}_5$, 423.1920, found 423.1917 $[\text{M}+\text{H}]^+$.

4.1.2.19. (Z)-3-(4'-(2-(2,6-Dimethylmorpholino)-2-oxoethoxy)-3'-methoxybenzylidene)-5-fluoroindolin-2-one (**4s**). Yellow solid, yield 83%; Mp: 246–248 °C; ¹H NMR (500 MHz, DMSO-*d*₆): δ 1.10 (d, *J* = 6.1 Hz, 3H), 1.10 (d, *J* = 6.1 Hz, 3H), 2.30 (t, *J* = 11.5 Hz, 1H), 2.73 (t, *J* = 10.9 Hz, 1H), 3.39–3.46 (m, 1H), 3.51–3.59 (m, 1H), 3.77 (d, *J* = 12.9 Hz, 1H), 3.85 (s, 3H), 4.18 (d, *J* = 12.8 Hz, 1H), 4.88 (d, *J* = 14.7 Hz, 1H), 5.01 (d, *J* = 14.7 Hz, 1H), 6.77–6.82 (m, 1H), 6.96–7.02 (m, 2H), 7.60 (dd, *J* = 2.4, 9.0 Hz, 1H), 7.78–7.84 (m, 2H), 8.66 (d, *J* = 1.7 Hz, 1H), 10.57 (s, 1H); ¹³C NMR (125 MHz, DMSO-*d*₆): δ 18.3, 18.6, 46.6, 49.7, 55.5, 66.2, 71.1, 71.3, 106.6 (d, *J*_{CF} = 25.2 Hz), 109.9 (d, *J*_{CF} = 7.9 Hz), 112.5, 114.3 (d, *J*_{CF} = 24.1 Hz), 115.4, 123.8, 127.0 (d, *J*_{CF} = 8.7 Hz), 127.3, 127.4, 136.4, 139.0, 148.0, 150.1, 157.9 (d, *J*_{CF} = 233.3 Hz), 165.3, 167.5; HRMS (ESI): *m/z* calcd. for C₂₄H₂₆FN₂O₅, 441.1826, found 441.1821 [M+H]⁺.

4.1.2.20. (Z)-5-Chloro-3-(4'-(2-(2,6-dimethylmorpholino)-2-oxoethoxy)-3'-methoxybenzylidene)indolin-2-one (**4t**). Yellow solid, yield 89%; Mp: 231–233 °C; ¹H NMR (500 MHz, DMSO-*d*₆): δ 1.10 (d, *J* = 6.2 Hz, 3H), 1.10 (d, *J* = 6.2 Hz, 3H), 2.30 (t, *J* = 11.9 Hz, 1H), 2.73 (t, *J* = 11.1 Hz, 1H), 3.39–3.47 (m, 1H), 3.51–3.59 (m, 1H), 3.77 (d, *J* = 12.9 Hz, 1H), 3.85 (s, 3H), 4.18 (d, *J* = 12.8 Hz, 1H), 4.88 (d, *J* = 14.7 Hz, 1H), 5.01 (d, *J* = 14.7 Hz, 1H), 6.83 (d, *J* = 8.2 Hz, 1H), 6.98 (d, *J* = 8.5 Hz, 1H), 7.20 (dd, *J* = 1.9, 8.2 Hz, 1H), 7.80 (d, *J* = 1.8 Hz, 1H), 7.84 (dd, *J* = 1.5, 8.6 Hz, 1H), 7.88 (s, 1H), 8.65 (d, *J* = 1.5 Hz, 1H), 10.68 (s, 1H); ¹³C NMR (125 MHz, DMSO-*d*₆): δ 18.3, 18.6, 46.6, 49.6, 55.4, 66.2, 71.1, 71.3, 110.5, 112.5, 115.5, 119.2, 122.9, 125.3, 127.3, 127.4 (2C), 127.5, 138.8, 139.3, 148.0, 150.1, 165.2, 167.2; HRMS (ESI): *m/z* calcd. for C₂₄H₂₆ClN₂O₅, 457.1530, found 457.1526 [M+H]⁺.

4.1.2.21. (Z)-5-Bromo-3-(4'-(2-(2,6-dimethylmorpholino)-2-oxoethoxy)-3'-methoxybenzylidene)indolin-2-one (**4u**). Orange solid, yield 83%; Mp: 237–238 °C; ¹H NMR (500 MHz, DMSO-*d*₆): δ 1.10 (d, *J* = 6.1 Hz, 3H), 1.10 (d, *J* = 6.1 Hz, 3H), 2.30 (t, *J* = 11.8

Hz, 1H), 2.73 (t, $J = 11.1$ Hz, 1H), 3.39–3.46 (m, 1H), 3.51–3.59 (m, 1H), 3.77 (d, $J = 12.9$ Hz, 1H), 3.85 (s, 3H), 4.18 (d, $J = 12.9$ Hz, 1H), 4.88 (d, $J = 14.7$ Hz, 1H), 5.01 (d, $J = 14.7$ Hz, 1H), 6.79 (d, $J = 8.2$ Hz, 1H), 6.98 (d, $J = 8.5$ Hz, 1H), 7.33 (dd, $J = 1.6, 8.2$ Hz, 1H), 7.84 (dd, $J = 1.5, 8.5$ Hz, 1H), 7.88 (s, 1H), 7.92 (d, $J = 1.3$ Hz, 1H), 8.65 (d, $J = 1.4$ Hz, 1H), 10.69 (s, 1H); ^{13}C NMR (125 MHz, DMSO- d_6): δ 18.3, 18.6, 46.6, 49.6, 55.5, 66.2, 71.1, 71.3, 111.1, 112.6, 113.0, 115.5, 122.0, 122.8, 127.4 (2C), 127.8, 130.3, 139.2, 139.3, 148.0, 150.1, 165.2, 167.1; HRMS (ESI): m/z calcd. for $\text{C}_{24}\text{H}_{26}\text{BrN}_2\text{O}_5$, 501.1005, found 501.1006 $[\text{M}+\text{H}]^+$.

4.1.2.22. (Z)-3-(4'-(2-(2,6-Dimethylmorpholino)-2-oxoethoxy)-3'-methoxybenzylidene)-5-methylindolin-2-one (**4v**). Orange solid, yield 90%; Mp: 214–215 °C; ^1H NMR (500 MHz, DMSO- d_6): δ 1.09 (d, $J = 6.1$ Hz, 3H), 1.09 (d, $J = 6.1$ Hz, 3H), 2.28 (s, 3H), 2.28–2.32 (m, 1H), 2.73 (dd, $J = 10.9, 13.0$ Hz, 1H), 3.41–3.44 (m, 1H), 3.51–3.57 (m, 1H), 3.77 (d, $J = 13.0$ Hz, 1H), 3.85 (s, 3H), 4.18 (d, $J = 13.0$ Hz, 1H), 4.87 (d, $J = 14.5$ Hz, 1H), 4.99 (d, $J = 14.5$ Hz, 1H), 6.71 (d, $J = 8.0$ Hz, 1H), 6.95 (d, $J = 8.6$ Hz, 1H), 6.98 (d, $J = 8.0$ Hz, 1H), 7.49 (s, 1H), 7.69 (s, 1H), 7.81 (dd, $J = 1.9, 8.6$ Hz, 1H), 8.65 (d, $J = 1.9$ Hz, 1H), 10.45 (s, 1H); ^{13}C NMR (125 MHz, DMSO- d_6): δ 18.3, 18.6, 20.8, 46.6, 49.7, 55.5, 66.2, 71.1, 71.3, 109.0, 112.5, 115.3, 119.7, 124.3, 125.4, 126.8, 127.7, 128.6, 129.6, 136.9, 138.0, 148.0, 149.6, 165.3, 167.5; HRMS (ESI): m/z calcd. for $\text{C}_{25}\text{H}_{29}\text{N}_2\text{O}_5$, 437.2076, found 437.2070 $[\text{M}+\text{H}]^+$.

4.2. Biological Evaluation

4.2.1. MTT assay

The cytotoxic activity of the compounds (**4a–v**) was determined using MTT assay. For preliminary screening, 1×10^4 cells per well were seeded in 100 μL DMEM, supplemented with 10% FBS in each well of 96-well microculture plates and incubated for 24 h at 37 °C in

a CO₂ incubator. Compounds **4a–v**, diluted to the desired concentrations (for preliminary screening; 20 µM concentration) in culture medium, were added to the wells with respective vehicle control. After 48 h of incubation, 10 µL MTT (3-(4,5-dimethylthiazol-2-yl)-2,5-diphenyl tetrazolium bromide) (5 mg mL⁻¹) was added to each well and the plates were further incubated at 37 °C for 4 h. Then, the supernatant from each well was carefully removed, formazan crystals were dissolved in 200 µL of DMSO and incubated at 37 °C for 10 min. The absorbance at 570 nm was measured on a spectrophotometer (SpectraMax, Molecular devices).

The compounds which exhibited >50% inhibition of cell viability at 20 µM in preliminary screening; were further selected to generate drug response curve (DRC). The compounds **4a–4v** and standard sunitinib with series of concentrations (6 serial concentrations; 20–0.625 µM); MTT assay was performed as described above. IC₅₀ values were determined from DRC plot by linear regression method: % cell inhibition (from control OD) *versus* different concentrations (µM). All the values were expressed as Mean ± SEM of three independent experiments in which each treatment was performed in triplicate wells.

4.2.2. Morphology

PC-3 cells were plated in 6 well culture plates with a cell density of 1 × 10⁵ cells/mL and allowed to adhere for overnight. The cells were incubated with the 1, 2, and 4 µM concentrations of the compound **4p**. After 48 h treatment, cells were observed for the morphological changes and photographs were taken under a phase contrast microscope (Nikon). For trypan blue assay, the cells were harvested by trypsinization, mixed with trypan blue (0.4 %), and loaded on to the haemocytometer to count the dead and viable cells. Each sample was assayed for triplicates.

4.2.3. *In vitro* Cell migration Assay/Wound healing assay

The wound-healing assay is a proven method to study *in vitro* cell migration. PC-3 cells (5×10^5 cells/well) were cultured in 6 well plates for 24 h. The confluent monolayers were then scratched with 200 μ L pipette tip. The wounded monolayers were washed twice with PBS to remove non-adherent cells. Then, media containing the different concentrations (1, 2, and 4 μ M) of the compound **4p** were added to each well. Cells which migrated across the scratched wound were photographed under the phase contrast microscope (Nikon) at 0, 24 and 48 h time interval after treatment. The cells that migrated to the wounded areas were counted using Nikon NIS elements software and the percentage of migrated cells in each experimental condition was calculated in comparison to control cells (DMSO exposed cells).

4.2.4. Effect on Structures of F-actin

PC-3 cells (5×10^5 cells/mL) were grown on cover slips in a 6 well plates for 24 h and were treated with 1, 2, and 4 μ M concentrations of the compound **4p**. After 12 h treatment, cells were washed with PBS and stained with rhodamine phalloidin (R-145, Life technologies), a red fluorescent dye that specifically stains F-actin structures [46]. Hoechst 33242 was used to stain the nucleus. Images were captured using confocal microscope. (Nikon)

4.2.5. Flow cytometry analysis

To determine the effect of compound **4p** on the cell cycle, PC-3 cells were seeded in 6 well plates at a density of 1×10^6 cells/well. After 24 h of incubation, cells were treated with compound **4p** in three different concentrations (1, 2 and 4 μ M). Cells treated with DMSO were used as control. 24 h after treatment, both floating and trypsinised cells were harvested and washed with PBS. Cells were fixed with 70% ethanol for 30 min at 4 °C. Then, cells were centrifuged (1200 rpm for 5 min), the supernatant was discarded and the pellet was washed with PBS and stained the cells with propidium iodide staining buffer (PI (200 μ g), 0.1% (v/v) Triton X-100, 2 mg DNase-free RNase A (Sigma) in 10 mL PBS) for 15 min at

ambient temperature in absence of light. Later, samples were analyzed for propidium iodide-DNA fluorescence from 10000 events by flow cytometry using BD-C6 accuri flow cytometer.

4.2.6. Hoechst staining

Human prostate cancer PC-3 cells were grown on cover slips in a 6 well plates (5×10^4 cells/well) and allowed to adhere for 24 h. The culture medium containing the compound **4p** with 1, 2, and 4 μM concentrations were added to the cells. After 24 h incubation, culture medium was removed; cells were washed with PBS and fixed with 4% paraformaldehyde solution at 4 °C for 10 min. Then, cells were washed twice with PBS and stained with Hoechst 33242 (5 $\mu\text{g}/\text{mL}$) for 30 min at room temp. The excess dye was removed by washing twice with PBS and cell suspensions were mounted on slides and were examined for morphological changes under confocal fluorescence microscope using 350 nm excitation and 460 nm emission (Nikon, magnification 40X).

4.2.7. Measurement of Mitochondrial Membrane Potential (MMP)

PC-3 cells were cultured in 6 well plates at a density of 5×10^5 cells/mL and allowed to grow over night. The cells were treated with 1, 2, and 4 μM concentrations of the compound **4p**. After 24 h incubation, the adherent cells were collected by trypsinsation, washed with PBS and resuspended in a solution of PBS containing Rhodamine-123 (10 $\mu\text{g}/\text{mL}$). After incubation for 30 min at room temperature, cells were washed twice with PBS and re-suspended in PBS. The samples were analyzed for Rhodamine123 fluorescence using spectrofluorometer.

4.2.8. Measurement of intracellular calcium

Intracellular Ca^{2+} concentration was determined in PC-3 cells using a reported method Thushara et al. [42]. The PC-3 cells (2×10^5 cells/mL) were plated in 24 well plates and allowed to adhere for overnight. The cells were treated with increasing doses (1, 2 and 4 μM) of the compound **4p** for a period of 24 h. After treatment, cells were incubated with 2 μM of fura-2/AM, a fluorescence Ca^{2+} indicator, for 1 h. The cells were then washed twice with Hanks' balanced saline solution containing 10 mM HEPES and 10 mM glucose. The images were captured using excitation/emission at 340 and 380 nm using fluorescence microscope (Nikon).

4.2.9. Annexin V-FITC/Propidium iodide dual staining assay

The Annexin V-FITC/propidium iodide dual staining assay was carried out using PC-3 cells, to quantify the percentage of apoptotic cells [43]. Briefly, PC-3 cells (1×10^6 /mL per well) were plated in six-well plates and allowed to grow for 24. Cells were treated with increasing concentrations of compound **4p** (1, 2 and 4 μM) for 24 h and were collected by trypsinisation. The collected cells were washed twice with ice-cold PBS, then incubated with 200 μL binding buffer containing 5 μL Annexin V-FITC, and then in 300 μL binding buffer containing 5 μL Propidium iodide (PI) for 5 min at room temperature in the dark. After 15 min incubation, cells were analysed for apoptosis using BD-c6 accuri flow-cytometer.

4.2.10. Western blotting

For western blotting, PC-3 cells were treated with compound **4p** for 24 h. Whole cell extracts were prepared using RIPA (Sigma-Aldrich, St. Louis, MO, USA). Western blotting analysis was performed using anti-Caspase-3 (rabbit, 1:1000, Santa Cruz, CA), anti-Bcl2 (rabbit, 1:1000, Santa Cruz, CA), anti-Bax (rabbit, 1:500, Santa Cruz, CA), anti- β -actin (rabbit, 1:1000, Santa Cruz, CA) and HRP-conjugated secondary antibodies (Santa Cruz, CA). The antigen-antibody complex was visualized with an ECL detection kit (Amersham Bioscience).

For subsequent antibody treatment, membranes were stripped in stripping buffer and re-probed with another antibody [47]. The immune blots were quantified by densitometry scanning with NIH ImageJ software.

Acknowledgements

K.R.S. and P.S. are thankful to DoP, Ministry of Chemicals & Fertilizers, Govt. of India, for the award of NIPER fellowship. NS gratefully acknowledges SERB, DST, Govt. of India for research grant (YSS-2015-001709).

5.0. References

- [1] R.L. Siegel, K.D. Miller, A. Jemal, Cancer statistics, 2015, *CA Cancer J. Clin.* 65 (2015) 5–29.
- [2] A. Millemaggi, R.J.K. Taylor, 3-Alkenyl-oxindoles: Natural products, pharmaceuticals, and recent synthetic advances in tandem/telescoped approaches, *Eur. J. Org. Chem.* 24 (2010) 4527–4547.
- [3] S. Peddibhotla, 3-Substituted-3-hydroxy-2-oxindole, an emerging new scaffold for drug discovery with potential anti-cancer and other biological activities, *Curr. Bioact. Compd.* 5 (2009) 20–38.
- [4] G.S. Singh, Z.Y. Desta, Isatins as privileged molecules in design and synthesis of spiro-fused cyclic frameworks, *Chem. Rev.* 112 (2012) 6104–6155.
- [5] C.V. Galliford, K.A. Scheidt, Pyrrolidinyl-spirooxindole natural products as inspirations for the development of potential therapeutic agents, *Angew. Chem. Int. Ed.* 46 (2007) 8748–8758.
- [6] G.H. Zheng, J.J. Shen, Y.C. Zhan, H. Yi, S.T. Xue, Z. Wang, X.Y. Ji, Z. R. Li, Design, synthesis and *in vitro* and *in vivo* antitumour activity of 3-benzylideneindolin-2-one

derivatives, a novel class of small-molecule inhibitors of the MDM2–p53 interaction, *Eur. J. Med. Chem.* 81 (2014) 277–288.

[7] G. Bhaskar, Y. Arun, C. Balachandran, C. Saikumar, P.T. Perumal, Synthesis of novel spirooxindole derivatives by one pot multicomponent reaction and their antimicrobial activity, *Eur. J. Med. Chem.* 51 (2012) 79–91.

[8] Y. Kia, H. Osman, R.S. Kumar, V. Murugaiyah, A. Basiri, S. Perumal, H.A. Wahab, C.S. Bing, Synthesis and discovery of novel piperidone-grafted mono- and bispirooxindole-hexahydropyrrolizines as potent cholinesterase inhibitors, *Biorg. Med. Chem.* 21(2013) 1696–1707.

[9] K. Huber, J. Schemies, U. Uciechowska, J.M. Wagner, T. Rumpf, F. Lewrick, R. Süß, W. Sippl, M. Jung, F. Bracher, Novel 3-arylideneindolin-2-ones as inhibitors of NAD⁺-dependent histone deacetylases (sirtuins), *J. Med. Chem.* 53 (2009) 1383–1386.

[10] A. Leoni, A. Locatelli, R. Morigi, M. Rambaldi, 2-Indolinone a versatile scaffold for treatment of cancer: a patent review (2008-2014), *Expert Opin. Ther. Pat.* 26 (2016) 149–173.

[11] C.R. Prakash, S. Raja, Indolinones as promising scaffold as kinase inhibitors: a review, *Mini. Rev. Med. Chem.* 12 (2012) 98–119.

[12] G.J. Roth, R. Binder, F. Colbatzky, C. Dallinger, R. Schlenker-Herceg, F. Hilberg, S.L. Wollin, R. Kaiser, Nintedanib: from discovery to the clinic, *J. Med. Chem.* 58 (2015) 1053–1063.

[13] R.J. Motzer, M.D. Michaelson, B.G. Redman, G.R. Hudes, G. Wilding, R.A. Figlin, M.S. Ginsberg, S.T. Kim, C.M. Baum, S.E. DePrimo, J.Z. Li, C.L. Bello, C.P. Theuer, D.J. George, B.I. Rini, Activity of SU11248, a multitargeted inhibitor of vascular endothelial growth factor receptor and platelet-derived growth factor receptor, in patients with metastatic renal cell carcinoma, *J. Clin. Oncol.* 24 (2006) 16–24.

- [14] H. Prenen, J. Cools, N. Mentens, C. Folens, R. Sciot, P. Schöffski, A.V. Oosterom, P. Marynen, M. Debiec-Rychter, Efficacy of the kinase inhibitor SU11248 against gastrointestinal stromal tumor mutants refractory to imatinib mesylate, *Clin. Cancer Res.* 12 (2006) 2622–2627.
- [15] J.J. Cui, M. McTigue, M. Nambu, M. Tran-Dube, M. Pairish, H. Shen, L. Jia, H. Cheng, J. Hoffman, P. Le, M. Jalaie, G.H. Goetz, K. Ryan, N. Grodsky, Y.L. Deng, M. Parker, S. Timofeevski, B.W. Murray, S. Yamazaki, S. Aguirre, Q. Li, H. Zou, J. Christensen, Discovery of a novel class of exquisitely selective mesenchymal epithelial transition factor (MET) protein kinase inhibitors and identification of the clinical candidate 2-(4-(1-(quinolin-6-ylmethyl)-1H-[1,2,3]triazolo[4,5-*b*]pyrazin-6-yl)-1H-pyrazol-1-yl)ethanol (PF-04217903) for the treatment of cancer, *J. Med. Chem.* 55 (2012) 8091–8109.
- [16] M. Haddach, J. Michaux, M.K. Schwaebe, F. Pierre, S.E. O'Brien, C. Borsan, J. Tran, N. Raffaele, S. Ravula, D. Drygin, A. Siddiqui-Jain, L. Darjania, R. Stansfield, C. Proffitt, D. Macalino, N. Streiner, J. Bliesath, M. Omori, J.P. Whitten, K. Anderes, W.G. Rice, D.M. Ryckman, Discovery of CX-6258. A potent, selective, and orally efficacious pan-Pim kinases inhibitor, *ACS Med. Chem. Lett.* 3 (2012) 135–139.
- [17] T.P. Cho, S.Y. Dong, F. Jun, F.J. Hong, Y.J. Liang, X. Lu, P.J. Hua, L.Y. Li, Z. Lei, H. Bing, Z. Ying, L.F. Qiong, F.B. Bei, L.L. Guang, G.A. Shen, S.G. Hong, S.W. Hong, M.X. Tai, Novel potent orally active multitargeted receptor tyrosine kinase inhibitors: Synthesis, structure-activity relationships, and antitumor activities of 2-indolinone derivatives, *J. Med. Chem.* 53 (2010) 8140–8149.
- [18] A.D. Jagtap, P.T. Chang, J.R. Liu, H.C. Wang, N.B. Kondekar, L.J. Shen, H.W. Tseng, G.S. Chen, J.W. Chern, Novel acylureidoindolin-2-one derivatives as dual Aurora B/FLT3 inhibitors for the treatment of acute myeloid leukemia, *Eur. J. Med. Chem.* 85 (2014) 268–288.

- [19] H.C. Wang, A.D. Jagtap, P.T. Chang, J.R. Liu, C.P. Liu, H.W. Tseng, G.S. Chen, J.W. Chern, Bioisosteric replacement of an acylureido moiety attached to an indolin-2-one scaffold with a malonamido or a 2/4-pyridinoylamido moiety produces a selectively potent Aurora-B inhibitor, *Eur. J. Med. Chem.* 84 (2014) 312–334.
- [20] C. Pergola, N. Gaboriaud-Kolar, N. Jestädt, S. König, M. Kritsanida, A.M. Schaible, H. Li, U. Garscha, C. Weinigel, D. Barz, K.F. Albring, O. Huber, A.L. Skaltsounis, O. Werz, Indirubin core structure of glycogen synthase kinase-3 inhibitors as novel chemotype for intervention with 5-lipoxygenase, *J. Med. Chem.* 57 (2014) 3715–3723
- [21] H.N. Bramson, J. Corona, S.T. Davis, S.H. Dickerson, M. Edelstein, S.V. Frye, R.T. Gampe, Jr., P.A. Harris, A. Hassell, W.D. Holmes, R.N. Hunter, K.E. Lackey, B. Lovejoy, M.J. Luzzio, V. Montana, W.J. Rocque, D. Rusnak, L. Shewchuk, J.M. Veal, D.H. Walker, L.F. Kuyper, Oxindole-based inhibitors of cyclin-dependent kinase 2 (CDK2): design, synthesis, enzymatic activities, and x-ray crystallographic analysis, *J. Med. Chem.* 44 (2001) 4339–4358.
- [22] P.B. Sampson, Y. Liu, B. Forrest, G. Cumming, S.W. Li, N.K. Patel, L. Edwards, R. Laufer, M. Feher, F. Ban, D.E. Awrey, G. Mao, O. Plotnikova, R. Hodgson, I. Beletskaya, J.M. Mason, X. Luo, V. Nadeem, X. Wei, R. Kiarash, B. Madeira, P. Huang, T.W. Mak, G. Pan, H.W. Pauls, The Discovery of Polo-like kinase 4 inhibitors: Design and optimization of spiro[cyclopropane-1,3'[3H]indol]-2'(1H)-ones as orally bioavailable antitumor Agents, *J. Med. Chem.* 58 (2015) 147–69.
- [23] K.R. Senwar, P. Sharma, T.S. Reddy, M.K. Jeengar, V.L. Nayak, V.G.M. Naidu, A. Kamal, N. Shankaraiah, Spirooxindole-derived morpholine-fused-1,2,3-triazoles: Design, synthesis, cytotoxicity and apoptosis inducing studies, *Eur. J. Med. Chem.* 102 (2015) 413–424.

- [24] K.R. Senwar, P. Sharma, S. Nekkanti, M. Sathish, A. Kamal, B. Sridhar, N. Shankaraiah, A one-pot 'click' reaction from spiro-epoxides catalyzed by Cu (i)-pyrrolidinyl-oxazole-carboxamide, *New J. Chem.* 39 (2015) 3973–3981.
- [25] M. Chouhan, K.R. Senwar, R. Sharma, V. Grover, V.A. Nair, Regiospecific epoxide opening: a facile approach for the synthesis of 3-hydroxy-3-aminomethylindolin-2-one derivatives, *Green Chem.* 13 (2011) 2553–2560.
- [26] M. Chouhan, K.R. Senwar, K. Kumar, R. Sharma, V.A. Nair, Catalytic C–H activation of arylacetylenes: A fast assembly of 3-(arylethynyl)-3-hydroxyindolin-2-ones using CuI/DBU, *Synthesis* 46 (2014) 195–202.
- [27] P. Sharma, K.R. Senwar, M.K. Jeengar, T.S. Reddy, V.G.M. Naidu, A. Kamal, N. Shankaraiah, H₂O-mediated isatin spiro-epoxide ring opening with NaCN: Synthesis of novel 3-tetrazolymethyl-3-hydroxy-oxindole hybrids and their anticancer evaluation, *Eur. J. Med. Chem.* 104 (2015) 11–24.
- [28] R.D. Taylor, M. MacCoss, A.D.G. Lawson, Rings in drugs, *J. Med. Chem.* 57 (2014) 5845–5859.
- [29] M. Andrs, J. Korabecny, D. Jun, Z. Hodny, J. Bartek, K. Kuca, Phosphatidylinositol 3-kinase (PI3K) and phosphatidylinositol 3-kinase-related kinase (PIKK) inhibitors: Importance of the morpholine ring, *J. Med. Chem.* 58 (2014) 41–71.
- [30] L. Sun, N. Tran, F. Tang, H. App, P. Hirth, G. McMahon, C. Tang, Synthesis and biological evaluations of 3-substituted indolin-2-ones: A novel class of tyrosine kinase inhibitors that exhibit selectivity toward particular receptor tyrosine kinases, *J. Med. Chem.* 41 (1998) 2588–2603.
- [31] X. Chen, T. Yang, A. Deivasigamani, M.K. Shanmugam, K.M. Hui, G. Sethi, M.L. Go, N'-Alkylaminosulfonyl analogues of 6-fluorobenzylideneindolinones with desirable

physicochemical profiles and potent growth inhibitory activities on hepatocellular carcinoma, *ChemMedChem* 10 (2015) 1548 – 1558.

[32] M. Nishikawa, H. Miyake, M. Fujisawa, Enhanced sensitivity to sunitinib by inhibition of Akt1 expression in human castration-resistant prostate cancer PC3 cells both in vitro and in vivo, *Urology* 85 (2015) 1215.e1–1215.e7.

[33] F. Yang, V. Jove, H. Xin, M. Hedvat, T.E. Van Meter, H. Yu, Sunitinib induces apoptosis and growth arrest of medulloblastoma tumor cells by inhibiting STAT3 and AKT signaling pathways, *Mol. Cancer Res.* 8 (2010) 35–45.

[34] E. Chinchar, K.L. Makey, J. Gibson, F. Chen, S.A. Cole, G.C. Megason, S. Vijayakumar, L. Miele, J.W. Gu, Sunitinib significantly suppresses the proliferation, migration, apoptosis resistance, tumor angiogenesis and growth of triple-negative breast cancers but increases breast cancer stem cells, *Vasc. Cell.* 6 (2014) 12.

[35] O. Belali, M. Ansari, H. Korashy, Sunitinib induces growth inhibition and apoptosis in breast cancer MDA-MB-231 cells through FOXO3a signaling pathway, *The FASEB Journal* 29(1 Supplement) (2015) 619–3.

[36] T.S. Reddy, H. Kulhari, V.G. Reddy, V. Bansal, A. Kamal, R. Shukla, Design, synthesis and biological evaluation of 1, 3-diphenyl-1*H*-pyrazole derivatives containing benzimidazole skeleton as potential anticancer and apoptosis inducing agents, *Eur. J. Med. Chem.* 101 (2015) 790–805.

[37] M.P. Sheetz, D. Felsenfeld, C.G. Galbraith, D. Choquet, Cell migration as a five-step cycle, *Biochem. Soc. Symp.* 65 (1999) 233–243.

[38] A. Kamal, T.S. Reddy, S. Polepalli, N. Shalini, V.G. Reddy, A.S. Rao, N. Jain, N. Shankaraiah, Synthesis and biological evaluation of podophyllotoxin congeners as tubulin polymerization inhibitors, *Bioorg. Med. Chem.* 22 (2014) 5466–5475.

- [39] D. Hanahan, R.A. Weinberg, Hallmarks of cancer: The next generation, *Cell* 144 (2011) 646–674.
- [40] A. Kamal, T.S. Reddy, M.V.P.S. Vishnuvardhan, V.D. Nimbarte, A.V. Subba Rao, V. Srinivasulu, N. Shankaraiah, Synthesis of 2-aryl-1,2,4-oxadiazolo-benzimidazoles: Tubulin polymerization inhibitors and apoptosis inducing agents, *Bioorg. Med. Chem.* 23 (2015) 4608–4623.
- [41] X.D. Wang, The expanding role of mitochondria in apoptosis, *Genes Dev.* 15 (2001) 2922–2933.
- [42] I. Kruman, Q. Guo, M.P. Mattson. Calcium and reactive oxygen species mediate staurosporine-induced mitochondrial dysfunction and apoptosis in PC12 cells, *J. Neurosci. Res.* 51 (1998) 293–308.
- [43] C. Praveen Kumar, T.S. Reddy, P.S. Mainkar, V. Bansal, R. Shukla, S. Chandrasekhar, H.M. Hügel, Synthesis and biological evaluation of 5,10-dihydro-11H-dibenzo[*b,e*][1,4]diazepin-11-one structural derivatives as anti-cancer and apoptosis inducing agents, *Eur. J. Med. Chem.* 108 (2016) 674–686.
- [44] A.G. Porter, R.U. Jänicke, Emerging roles of caspase-3 in apoptosis, *Cell Death Differ.* 6 (1999) 99–104.
- [45] S. Shrivastava, P. Kulkarni, D. Thummuri, M.K. Jeengar, V.G.M. Naidu, M. Alvala, G.B. Reddy, S. Ramakrishna, Piperlongumine, an alkaloid causes inhibition of PI3 K/Akt/mTOR signaling axis to induce caspase-dependent apoptosis in human triple-negative breast cancer cells, *Apoptosis* 19 (2014) 1148–1164.
- [46] B. Janji, L. Vallar, Z.Al. Tanoury, F. Bernardin, G. Vetter, E. Schaffner-Reckinger, G. Berchem, E. Friederich, S. Chouaib, The actin filament cross-linker L-plastin confers resistance to TNF-alpha in MCF-7 breast cancer cells in a phosphorylation-dependent manner, *J. Cell Mol. Med.* 14 (2010), 1264–1275.

[47] D. Thummuri, M.K. Jeengar, S. Srivastava, A. Areti, V.G. Yerra, S. Yamjala, P. Komirishetty, V.G.M. Naidu, A. Kumar, R. Sistla, *Boswellia ovalifoliolata* abrogates ROS mediated NF- κ B activation, causes apoptosis and chemosensitization in Triple Negative Breast Cancer cells, *Environ. Toxicol. Pharmacol.* 38 (2014) 58–70.

ACCEPTED MANUSCRIPT

Table 1. IC₅₀ Values^a (in μ M) for compounds **4a–v** on selected human cancer cell lines

Figure 1. Representative examples of 3-alkenyl-indolin-2-one drugs **1–3** and rationale for the designed target compounds **4a–v**.

Figure 2. Schematic representation of characteristic NOEs of compound **4v**.

Figure 3. (a) Effect of compound **4p** on morphological features and cell viability of PC-3 cells. (b) The percentage of viable cells present after 48 h was measured in compound **4p** treated cells by trypan blue assay.

Figure 4. Effect of compound **4p** on migration potential of PC-3 cells: (a) PC-3 cells were exposed to the compound **4p** and scratches were done with sterile 200 μ L pipette. The images were captured at 0, 24, and 48 h in an *in vitro* wound healing assay. (b) The no. of cells migrated in to the wound area was quantified using Nikon NIS elements software.

Figure 5. Effect of compound on structures of F-actin. PC-3 cells were treated with different concentrations of the compound **4p** and stained for actin filaments with rhodamine phalloidin (red). Hoechst 33242 was used to stain the nucleus (blue).

Figure 6. Effect of compound **4p** on cell cycle progression of PC-3 cells. Cells were treated with **4p** and harvested after 24 h. The cells were fixed with ethanol, stained with propidium iodide and analyzed by BD-C6 accuri flow-cytometer. For each sample, 10,000 cells were used for sorting.

Figure 7. Compound **4p** induced nuclear morphological changes of PC-3 cells after treatment for 24 h.

Figure 8. Effect of compound **4p** on mitochondrial membrane potential ($D\Psi_m$): The compound treated PC3 cells were stained with rhodamine 123 and the intensity of rhodamine

123 fluorescence in each sample was analyzed by spectrofluorometer. Data were mean \pm SD of three independent experiments.

Figure 9. Effect of compound **4p** on intracellular Ca^{2+} levels. PC-3 cells were treated with different concentrations (1, 2 and 4 μM) of compound **4p** for 24 h and stained with Fura-2 AM to measure the intracellular calcium levels. Images were captured with fluorescent microscope.

Figure 10. Effect of compound **4p** on induction of apoptosis in PC-3 cells after 24 h. The compound **4p** treated cells stained with Annexin V-FITC/PI and analysed for apoptosis using BD c6 accuri flowcytometer. The 10,000 cells from each sample were analysed by flowcytometry. The percentage of cells positive for Annexin V-FITC and/or Propidium iodide is reported inside the quadrants. Cells in the lower left quadrant (Q1-LL: AV-/PI-): live cells; lower right quadrant (Q1-LR: AV+/PI-): early apoptotic cells; upper right quadrant (Q1-UR: AV+/PI +): late apoptotic cells and upper left quadrant (Q1-UL: AV-/PI+): necrotic cells.

Figure 11. Western blotting analysis of compound **4p** after treatment with 1.25, 2.5 and 5 μM concentrations for 24 h using caspase-3, Bcl2 and Bax in PC-3 cells. The western blot shown here are representative of three independent experiments with similar results. The immune blots were quantified by densitometry scanning with NIH ImageJ software. Histogram represents relative density data of the western blot, from all experiments, shown in % fold change \pm SEM.

Scheme 1. Synthesis of (Z)-3'-(3-methoxy-4'-(2-amino-2-oxoethoxy)-benzylidene)indolin-2-one derivatives **4a-v**.

Table 1. IC₅₀ Values^a (in μM) for compounds **4a–v** on selected human cancer cell lines

Compound	PC-3 ^b	DU-145 ^c	BT-549 ^d	MDA-MB-231 ^e	RWPE-1 ^f
4a	5.97±0.8	5.75±0.8	8.87±0.6	9.78±0.3	81.75±5.4
4b	>20	>20	>20	>20	NT
4c	>20	>20	>20	>20	NT
4d	>20	>20	>20	>20	NT
4e	>20	>20	>20	>20	NT
4f	6.97±0.6	6.63±0.5	>20	19.32±1.4	78.14±7.7
4g	>20	>20	>20	>20	NT
4h	6.40±0.5	6.50±0.7	4.69±0.5	12.61±0.4	87.61±1.1
4i	2.39±0.3	2.69±0.4	13.69±0.9	14.91±0.9	90.99±2.3
4j	>20	>20	>20	>20	NT
4k	>20	>20	>20	>20	NT
4l	>20	>20	>20	>20	NT
4m	>20	>20	>20	>20	NT
4n	>20	>20	>20	>20	NT
4o	>20	>20	>20	>20	NT
4p	1.89±0.6	1.94±0.2	7.17±0.3	6.35±0.3	>100
4q	3.08±0.3	3.40±0.4	9.87±0.5	5.81±0.4	23.15±6.0
4r	>20	>20	>20	>20	NT
4s	>20	>20	>20	>20	NT
4t	2.62±0.2	3.10±0.6	>20	17.63±0.8	>100
4u	>20	>20	>20	>20	NT
4v	>20	>20	>20	>20	NT
Sunitinib	19.6±3.0	16.4±0.5	15.5±0.5	7.4±0.5	23.0±1.2

^a 50% Inhibitory concentration after 48 h of drug treatment; ^{b, c} Human prostate cancer; ^{d, e} Human breast

cancer; ^f Normal human prostate epithelial cell line; and NT - Not tested. All the values are expressed as Mean

± SEM of three independent experiments in which each treatment was performed in triplicate wells.

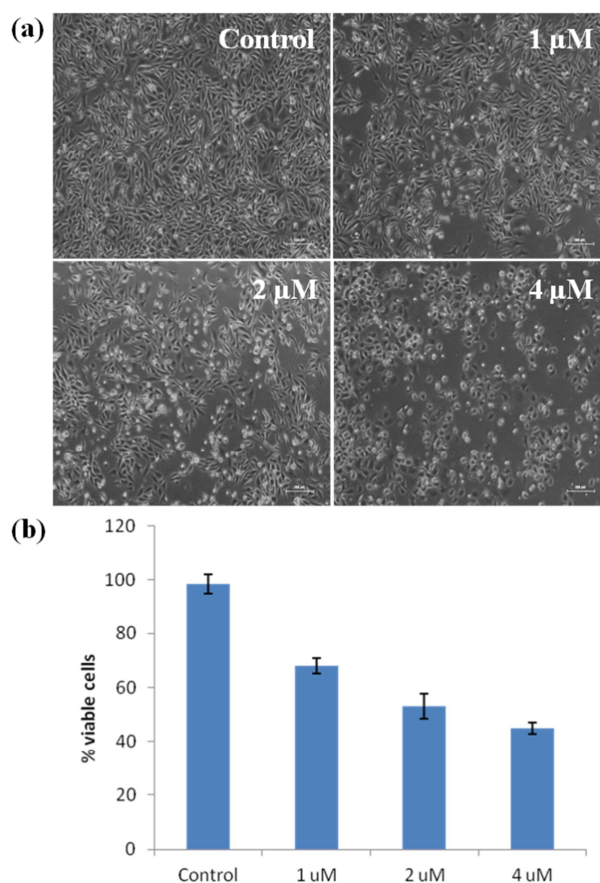


Figure 3. (a) Effect of compound **4p** on morphological features and cell viability of PC-3 cells. (b) The percentage of viable cells present after 48 h was measured in compound **4p** treated cells by trypan blue assay.

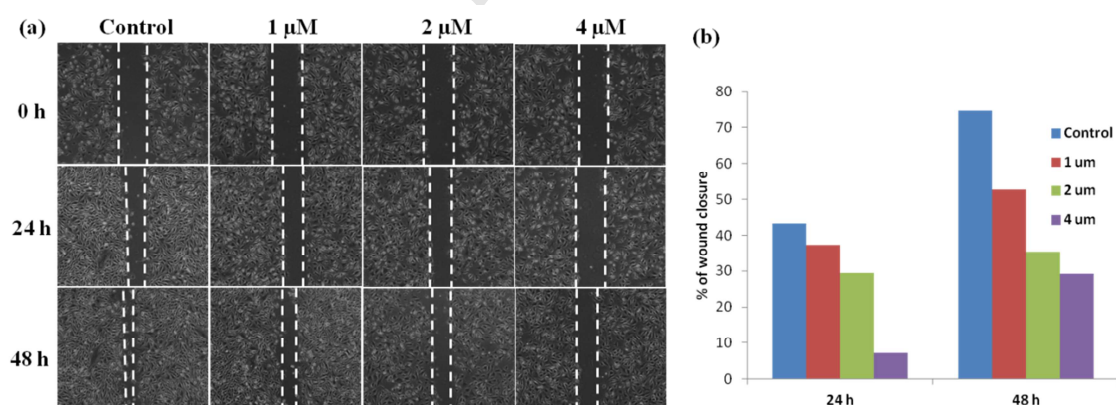


Figure 4. Effect of compound **4p** on migration potential of PC-3 cells: (a) PC-3 cells were exposed to the compound **4p** and scratches were done with sterile 200 μL pipette. The images

were captured at 0, 24, and 48 h in an *in vitro* wound healing assay. (b) The no. of cells migrated in to the wound area was quantified using Nikon NIS elements software.

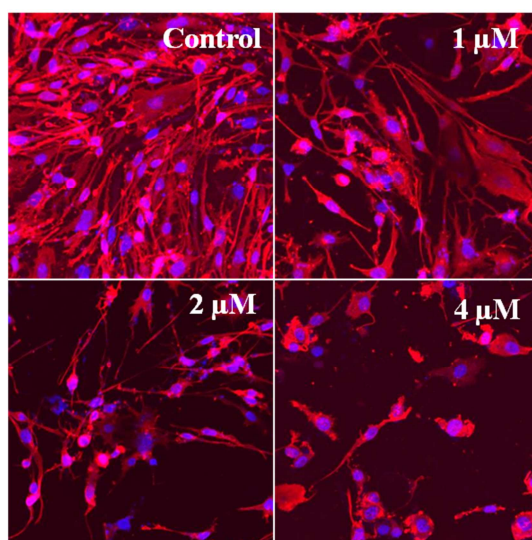


Figure 5. Effect of compound on structures of F-actin. PC-3 cells were treated with different concentrations of the compound **4p** and stained for actin filaments with rhodamine phalloidin (red). Hoechst 33242 was used to stain the nucleus (blue).

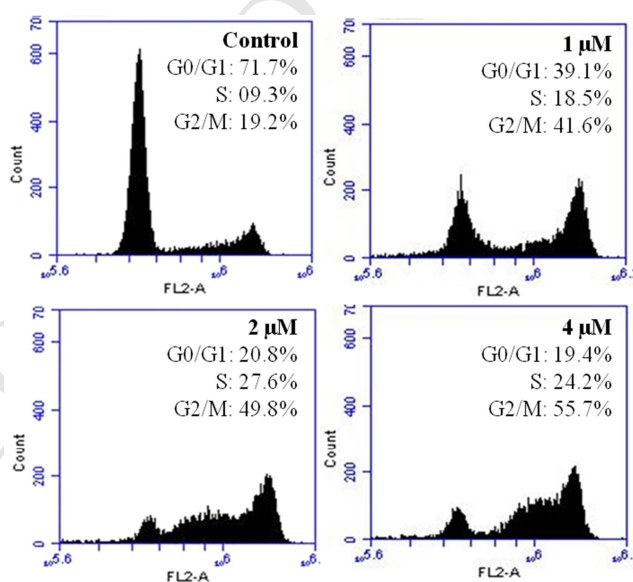


Figure 6. Effect of compound **4p** on cell cycle progression of PC-3 cells. Cells were treated with **4p** and harvested after 24 h. The cells were fixed with ethanol, stained with propidium

iodide and analyzed by BD-C6 accuri flow-cytometer. For each sample, 10,000 cells were used for sorting.

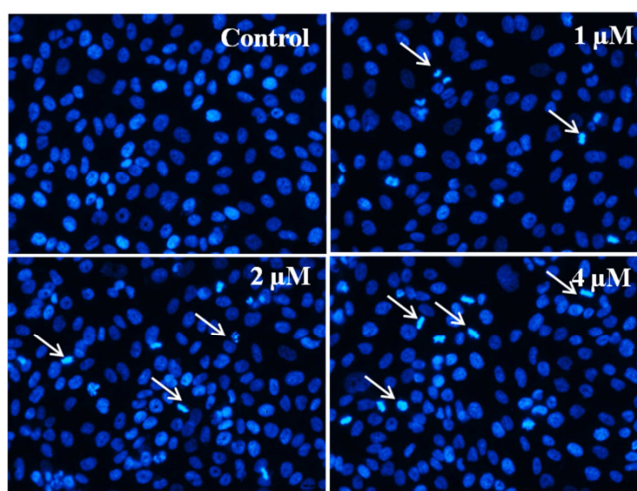


Figure 7. Compound **4p** induced nuclear morphological changes of PC-3 cells after treatment for 24 h.



Figure 8. Effect of compound **4p** on mitochondrial membrane potential ($\Delta\Psi_m$): The compound treated PC3 cells were stained with rhodamine 123 and the intensity of rhodamine 123 fluorescence in each sample was analyzed by spectrofluorometer. Data were mean \pm SD of three independent experiments.

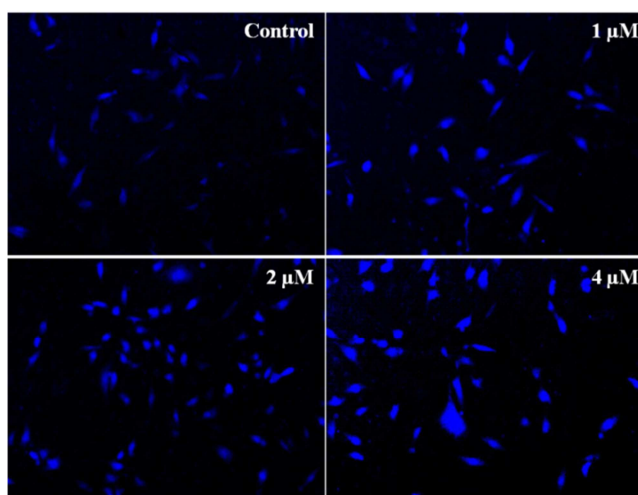


Figure 9. Effect of compound **4p** on intracellular Ca^{2+} levels. PC-3 cells were treated with different concentrations (1, 2 and 4 μM) of compound **4p** for 24 h and stained with Fura-2 AM to measure the intracellular calcium levels. Images were captured with fluorescent microscope.

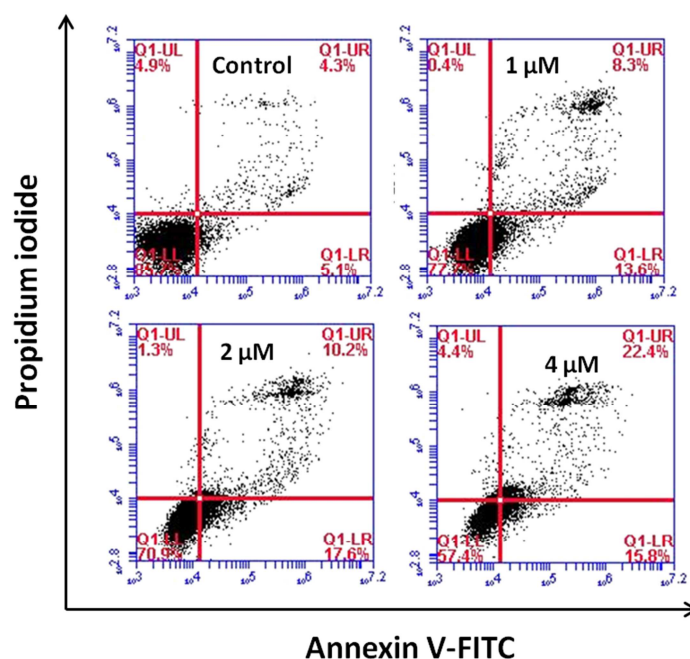


Figure 10. Effect of compound **4p** on induction of apoptosis in PC-3 cells after 24 h. The compound **4p** treated cells stained with Annexin V-FITC/PI and analysed for apoptosis using BD c6 accuri flowcytometer. The 10,000 cells from each sample were analysed by flowcytometry. The percentage of cells positive for Annexin V-FITC and/or Propidium

iodide is reported inside the quadrants. Cells in the lower left quadrant (Q1-LL: AV-/PI-): live cells; lower right quadrant (Q1-LR: AV+/PI-): early apoptotic cells; upper right quadrant (Q1-UR: AV+/PI +): late apoptotic cells and upper left quadrant (Q1-UL: AV-/PI+): necrotic cells.

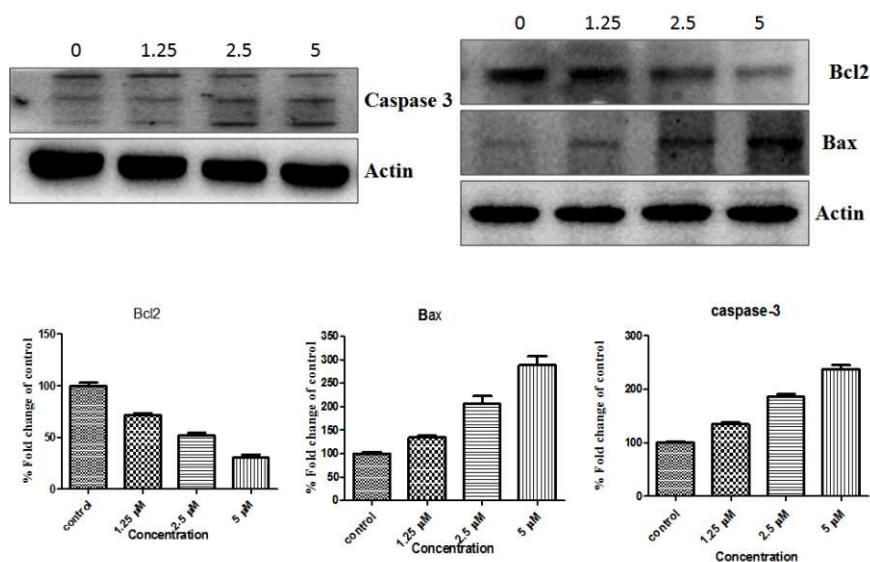
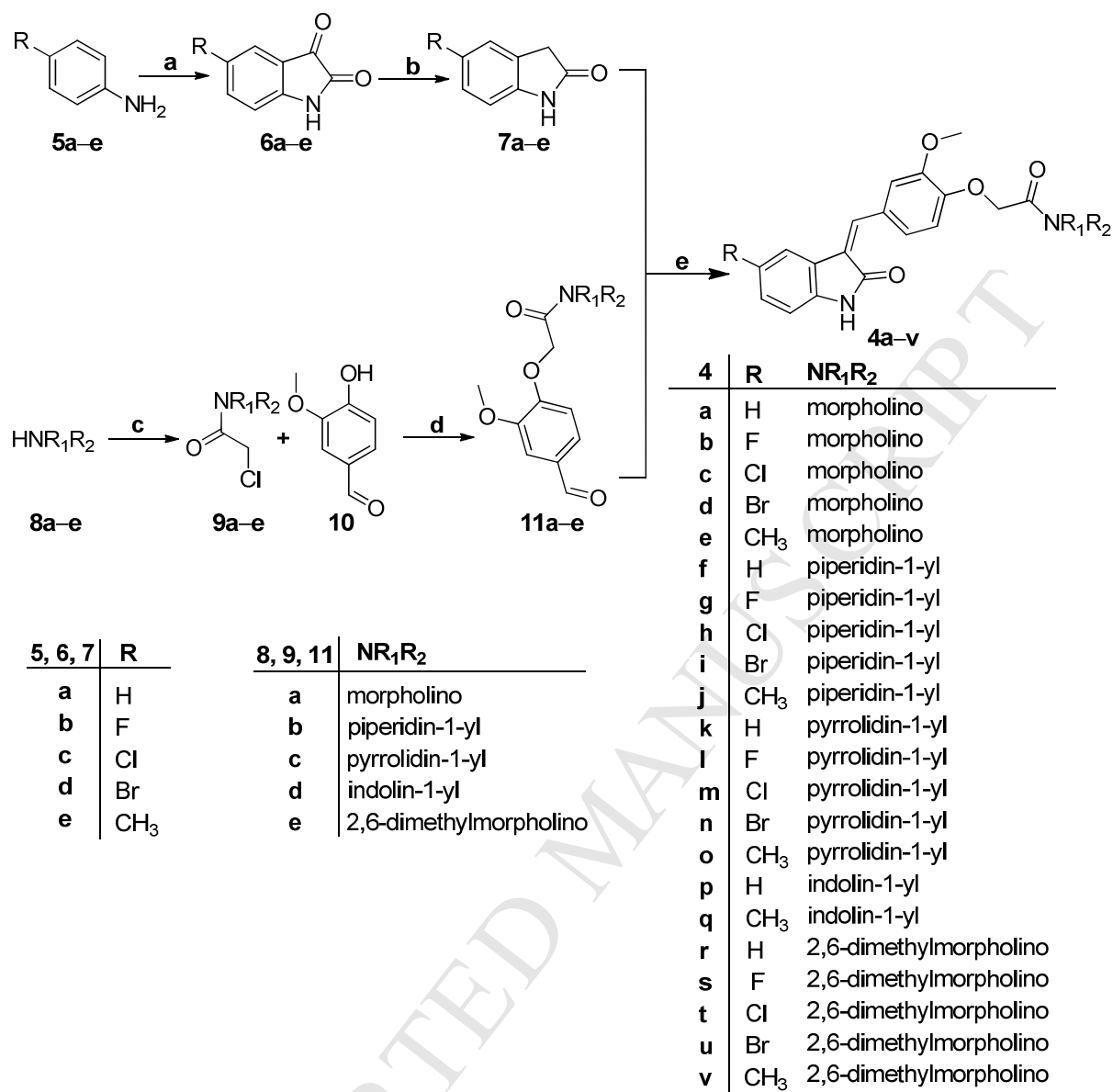


Figure 11. Western blotting analysis of compound **4p** after treatment with 1.25, 2.5 and 5 μ M concentrations for 24 h using caspase-3, Bcl2 and Bax in PC-3 cells. The western blot shown here are representative of three independent experiments with similar results. The immune blots were quantified by densitometry scanning with NIH ImageJ software. Histogram represents relative density data of the western blot, from all experiments, shown in % fold change \pm SEM.



Scheme 1. Synthesis of (Z)-3'-(3-methoxy-4'-(2-amino-2-oxoethoxy)-benzylidene)indolin-2-one derivatives **4a–v**; Reagents and conditions: (a) i) chloral hydrate, NH₂OH.HCl, 2N HCl, Na₂SO₄, H₂O, 70 °C; ii) Conc. H₂SO₄, 70 °C; (b) NH₂NH₂.H₂O, KOH, ethylene glycol, 110–130 °C, 2–3 h; (c) chloro-acetyl chloride, neat, 0 °C–r.t., 0.5–1 h; (d) K₂CO₃, acetonitrile, reflux, 5–6 h; or K₂CO₃, DMF, 0 °C–r.t., 6–8 h (e) piperidine (cat.), ethanol, reflux, 6–12 h.

Research Highlights

- (Z)-3-(3'-methoxy-4'-(2-amino-2-oxoethoxy)benzylidene)indolinones were synthesized.
- Test compound **4p** induced apoptosis, G2/M cell cycle arrest and disrupted F-actin.
- **4p** inhibited cell migration, collapse of the DΨm and increased levels of Ca²⁺.
- **4p** led to activation of caspase-3, changes in expression of Bax and Bcl-2 proteins.